

THE EFFECTS OF Fe II NON-LTE ON NOVA ATMOSPHERES AND SPECTRA

PETER H. HAUSCHILDT

Department of Physics and Astronomy, Arizona State University, Box 871504, Tempe, AZ 85287-1504; yeti@sara.la.asu.edu

E. BARON

Department of Physics and Astronomy, University of Oklahoma, 440 W. Brooks, Room 131, Norman, OK 73019-0225;
 baron@phyast.nhn.uoknor.edu

SUMNER STARRFIELD

Department of Physics and Astronomy, Arizona State University, Box 871504, Tempe, AZ 85287-1504; starrfie@hydro.la.asu.edu

AND

FRANCE ALLARD

Department of Physics, Wichita State University, Wichita, KS 67260-0032; allard@mugem.physics.twsu.edu

Received 1995 August 4; accepted 1995 November 8

ABSTRACT

The atmospheres of novae at early times in their outbursts are very extended, expanding shells with low densities. Models of these atmospheres show that non-LTE effects are very important and must be included in realistic calculations. We have, therefore, been improving our atmospheric studies by increasing the number of ions treated in non-LTE. One of the most important ions is Fe II, which has a complex structure and numerous lines in the observable spectrum. In this paper we investigate non-LTE effects for Fe II for a wide variety of parameters. We use a detailed Fe II model atom with 617 level and 13,675 primary lines, treated using a rate-operator formalism. We show that the radiative transfer equation in nova atmospheres *must* be treated with sophisticated numerical methods and that simple approximations, such as the Sobolev method, *cannot* be used because of the large number of overlapping lines in the comoving frame.

Our results show that the formation of the Fe II lines is strongly affected by non-LTE effects. For low effective temperatures, $T_{\text{eff}} < 20,000$ K, the optical Fe II lines are most influenced by non-LTE effects, while for higher T_{eff} the UV lines of Fe II are very strongly affected by non-LTE. The departure coefficients are such that Fe II tends to be overionized in non-LTE when compared to LTE. Therefore, Fe II non-LTE must be included with sophisticated radiative transfer in nova atmosphere models in order to analyze observed nova spectra reliably. Finally, we show that the number of wavelength points required for the Fe II non-LTE model atmosphere calculations can be reduced from 90,000 to about 30,000 without changing the results if we choose a sufficiently dense UV wavelength grid.

Subject headings: novae, cataclysmic variables — radiative transfer — stars: atmospheres

1. INTRODUCTION

The detailed modeling of early nova atmospheres and spectra has made significant progress over the last few years (see Hauschildt et al. 1992, 1995). Although the fits of synthetic spectra computed from model atmospheres to observed nova spectra is in general satisfactory (Hauschildt et al. 1994a, b), there are still a number of discrepancies between synthetic and observed nova spectra. In particular, in the “prenebular” phase of the nova evolution, when the effective temperature of the nova atmosphere is about 20,000–30,000 K, the fits to the Fe II lines in the UV spectral region (from 1000 to 3500 Å) become much worse than fits obtained in the earlier “optically thick wind” ($T_{\text{eff}} \approx 10,000$ –20,000 K) phase. In general, we have found that the lines of Fe II are too strong in the synthetic spectra for the prenebular phase when compared to the observations. However, the same Fe II lines and “clusters” of lines (i.e., groups of lines very close in wavelength) are reproduced well in models for the optically thick wind phase. In this paper, we show that these problems can be resolved by including a detailed non-LTE treatment of the important Fe II ion both in the nova model atmosphere calculations and the synthetic spectra.

The basic physical background of the formation of early nova spectra has been discussed in detail by Hauschildt et

al. (1995, hereafter Paper I). One of their most important results is that the formation of early nova spectra is extremely complex and that it cannot be described or modeled accurately using simple approximations. Nova spectra are formed in an environment which has an enormous density of lines, i.e., many thousands of spectral lines overlap in the comoving frame and, in addition, continuum absorption and scattering processes are important. *Therefore, the simple Sobolev approximation cannot be used to replace an accurate solution of the radiative transfer equation* (Baron, Hauschildt, & Mezzacapa 1995).

In our previous studies, we have found that non-LTE effects are also very important for the formation of early nova spectra. This means that multilevel non-LTE rate equations must be solved for a number of species self-consistently with the radiative transfer and energy equations. The effects of line blanketing and the differential velocity field of the expanding nova shell must also be included for an accurate treatment of the emergent radiation. So far, we have included only a limited number of the important species in full non-LTE; for the remaining species and spectral lines, we had to use LTE occupation numbers. An approximate treatment of line scattering was made in order to keep the nova atmosphere problem technically feasible. We have found that all species treated in

non-LTE show significant deviations from LTE in both their ionization balance and their line formation processes. Therefore, it is important to investigate the non-LTE effects of one of the most important ions (in terms of line opacity) found in nova atmospheres, the Fe II ion.

Hauschildt & Baron (1995, hereafter HB95) have used the numerical method developed by Hauschildt (1993, hereafter, H93) for non-LTE calculations with a very detailed model atom of Fe II. In this paper we will apply this method to nova model atmospheres and discuss the results and implications for the analysis of early nova spectra.

In the following section, we will describe briefly the Fe II model atom and the basic features of nova model atmospheres (details can be found in Paper I and HB95). We will then discuss the results we have obtained for representative nova model atmospheres, in particular the effects of Fe II non-LTE on the ionization balance and the formation of the Fe II lines. We conclude with a summary and discussion.

2. METHODS AND MODELS

2.1. Radiative Transfer

In the Lagrangian frame (“comoving frame”), the special relativistic equation of radiative transfer is given by (Mihalas & Weibel-Mihalas 1984)

$$\begin{aligned} \gamma(\mu + \beta) \frac{\partial I}{\partial r} + \frac{\partial}{\partial \mu} \left\{ \gamma(1 - \mu^2) \left[\frac{(1 + \beta\mu)}{r} - \gamma^2(\mu + \beta) \frac{\partial \beta}{\partial r} \right] I \right\} \\ - \frac{\partial}{\partial \nu} \left\{ \gamma \left[\frac{\beta(1 - \mu^2)}{r} + \gamma^2 \mu(\mu + \beta) \frac{\partial \beta}{\partial r} \right] \nu I \right\} \\ + \gamma \left\{ \frac{2\mu + \beta(3 - \mu^2)}{r} + \gamma^2(1 + \mu^2 + 2\beta\mu) \frac{\partial \beta}{\partial r} \right\} I \\ = \tilde{\eta} - \chi I. \end{aligned} \quad (1)$$

Here r is the radius, μ is the cosine of the angle between a ray and the direction normal to the surface, ν is the frequency, and $I = I(r, \mu, \nu)$ denotes the specific intensity at radius r and frequency ν in the direction $\arccos \mu$ in the Lagrangian frame. The matter velocity $v(r)$ is measured in units of the speed of light c : $\beta(r) = v(r)/c$, and γ is given by $\gamma(r) = 1/(1 - \beta^2)^{1/2}$. The sources of radiation present in the matter are described by the emission coefficient $\tilde{\eta} = \tilde{\eta}(r, \nu)$, and $\chi = \chi(r, \nu)$ is the extinction coefficient.

We solve equation (1) using an operator splitting method with a nonlocal band-matrix approximate Λ -operator (Hauschildt 1992; Hauschildt, Störzer, & Baron 1994c). As shown by Bath & Shaviv (1976), we can safely neglect the *explicit* time dependences and *partial* time derivatives $\partial/\partial t$ in the radiative transfer because the radiation flow timescale is much smaller than the timescale of the evolution of the nova outburst (even in the fireball stage). However, the advection and aberration terms must be retained in order to obtain a physically consistent solution (Mihalas & Weibel-Mihalas 1984). This approach is also consistent with the equation of radiation hydrodynamics in the time-independent limit (Mihalas & Weibel-Mihalas 1984; Baron et al. 1995). We neither neglect the Lagrangian time derivative $D/Dt = \partial/\partial t + v \partial/\partial r$ nor assign an ad hoc value to D/Dt as done by Eastman & Pinto (1993). The latter two assumptions lead to physical inconsistencies with the equations of radiation hydrodynamics (e.g., they do not lead to the correct equations for a steady state stellar wind). Our

approach is physically self-consistent because it includes the important advection and aberration terms in both the nongray radiative transfer and the radiative energy equations. The *only* term that we neglect is the *explicit* time dependence, which is a very good approximation in nova and supernova atmospheres (Baron et al. 1995).

Although our method is much more complicated than ad hoc assumptions for D/Dt (because of the additional terms in the equations that must be handled that break the symmetry of the characteristics of the radiative transfer equation), its results are much more reliable than those of simpler methods. In addition, the solution of the correct set of radiative transfer and energy equations in the comoving frame is no more time consuming than the solution of the corresponding static problem. This is because of our use of a nonlocal approximate Λ -operator.

2.2. Treatment of Spectral Lines

The physical conditions prevailing in nova atmospheres are such that a large number of spectral lines are present in the line-forming regions. Therefore, the simple Sobolev approximation *cannot* be used because many lines of comparable strength overlap (see Paper I). This means that the basic assumptions required to derive the Sobolev approximation are not valid. We demonstrate this in Figure 1a in which we plot the number of lines that are stronger than the local bound-free continuum and that lie within a ± 2 Doppler width wavelength interval around each wavelength point in the comoving frame. This graph is for a nova atmosphere with an effective temperature of 20,000 K, solar abundances, and a microturbulent or statistical velocity of $\xi = 2 \text{ km s}^{-1}$. In the UV, the number of overlapping strong lines at each wavelength point is typically larger than 10; in some regions, as many as 60 strong lines lie within 2 Doppler widths. Even in some regions of the optical spectral range, the number of overlapping lines can be as high as 10 or more. In Figure 1b we show that the situation becomes much worse for weaker lines (lines that are stronger than 10^{-4} of the local bound-free continuum must be included in nova atmosphere models; see Paper I). Now more than 1000 lines (all of comparable strength) in the UV and around 100 lines in the optical can overlap at each wavelength point. This shows that the Sobolev approximation cannot be used in modeling nova atmospheres. Therefore, we solve the full radiative transfer equation for all lines.

3. THE Fe II MODEL ATOM

We take the data needed to construct our model atom from the compilation of Kurucz (1994), whose long-term project to provide accurate atomic data for modeling stellar atmospheres is an invaluable service to the scientific community. For our current model atom, we have kept terms up to the ^2H term, which corresponds to the first 29 terms of Fe II. Within these terms, we include all observed levels that have observed b - b transitions with $\log gf > -3.0$ as non-LTE levels (where g is the statistical weight of the lower level and f is the oscillator strength of the transition). This leads to a model atom with 617 levels and 13,675 “primary” transitions which we treat in detailed non-LTE. We solve the complete bound-free and bound-bound radiative transfer and rate equations for all these levels and include all radiative rates of the primary lines. In addition, we treat the opacity and emissivity for the remaining nearly

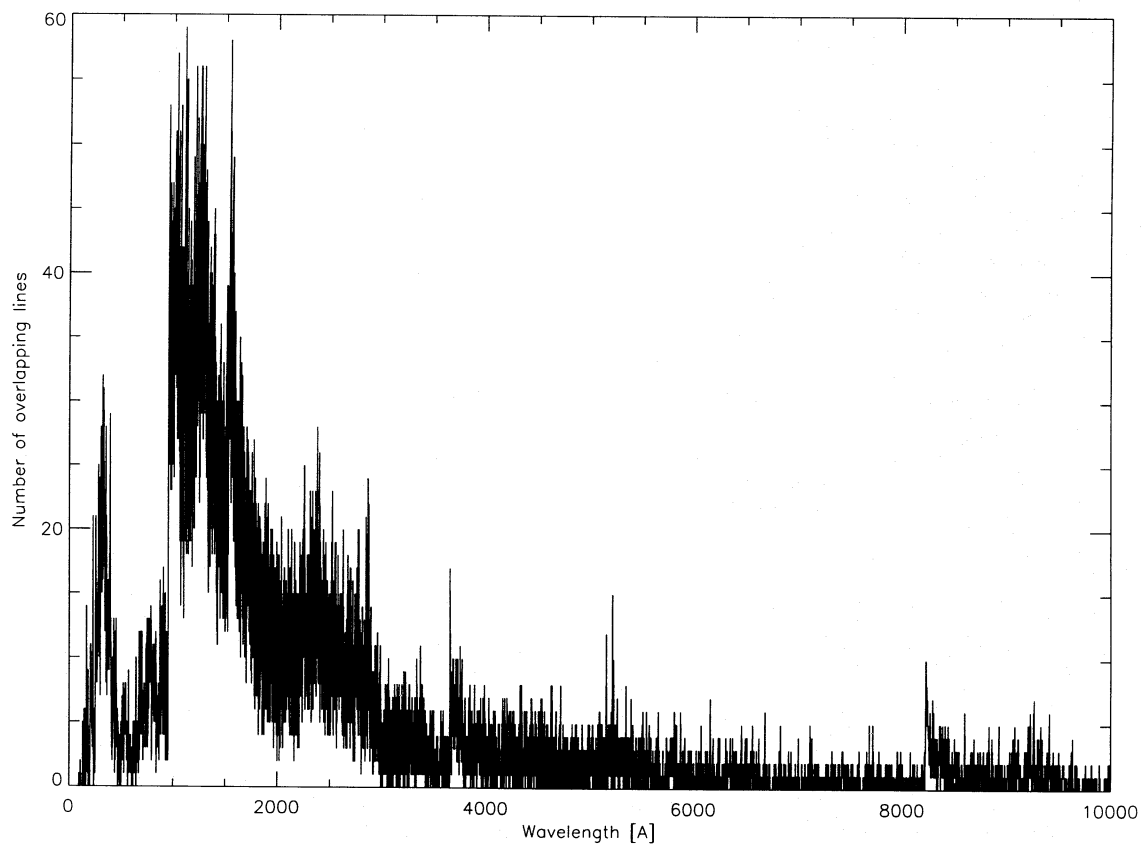


FIG. 1a

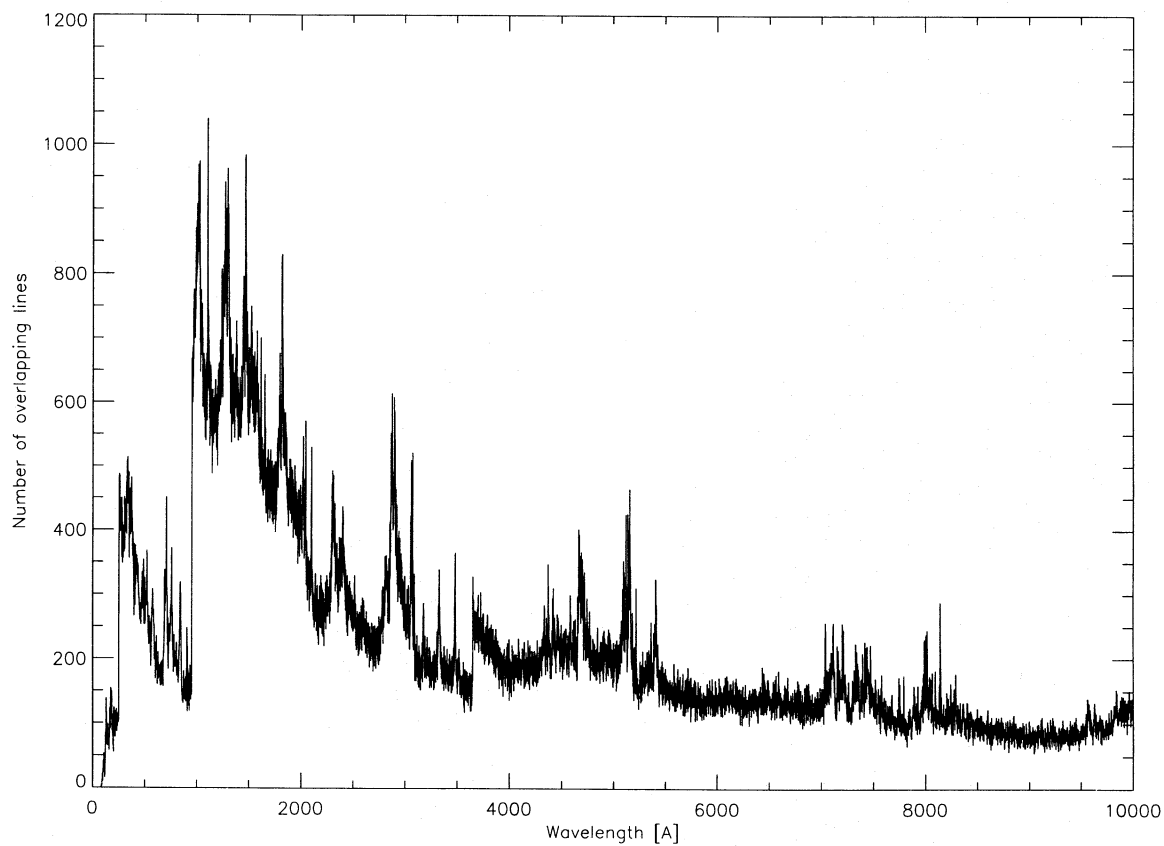


FIG. 1b

FIG. 1.—The number of overlapping lines in the comoving frame for a nova atmosphere model with $T_{\text{eff}} = 20,000$ K. We show the number of lines that lie within a ± 2 Doppler width interval at each wavelength point. In (a), only lines that are stronger than the local bound-free continuum are included, whereas in (b) all lines that are stronger than 10^{-4} times the local bound-free continuum are included. We have used a microturbulent velocity of $\xi = 2 \text{ km s}^{-1}$ in this calculation.

1.2×10^6 “secondary” bound-bound transitions in non-LTE, if one level of a secondary transition is included in our detailed model. We give a detailed description of the Fe II line treatment below.

3.1. Photoionization Rates

Detailed photoionization rates for Fe II have yet to be published, although this is one of the goals of the iron project. Thus, we have taken the results of the Hartree Slater central field calculations of Reilman & Manson (1979) to scale the ground-state photoionization rate and then have used a hydrogenic approximation for the energy variation of the cross section. Although these rates are only very rough approximations, they are useful for initial calculations. For the conditions of the test cases we consider in this paper, the exact values of the bound-free cross sections are not important for the opacities (which are dominated by known bound-bound transitions of Fe II and other species), but they do have an influence on the actual bound-free rates. This is, of course, unimportant for the computational method which we use, and the bound-free cross sections can be changed easily when better data become available.

3.2. Collisional Rates

For collisional rates, we have had to make rather rough approximations using semiempirical formulae. We have calculated bound-free collisional rates using the semiempirical formula of Drawin (1961). The bound-bound collisional rates are approximated by the semiempirical formula of Allen (1973) and, for permitted transitions, we use Von Regemorter’s formula (Van Regemorter 1962). While the collisional rates are important in stellar atmospheres with high electron densities, they are nearly negligible when compared to the radiative rates in the low-density envelopes of novae. If better collisional cross sections become available, they can be incorporated very easily.

3.3. Computational Method

The large number of transitions of the Fe II ion that have to be included in realistic models of the Fe II non-LTE line formation require an efficient method for the numerical solution of the multilevel non-LTE radiative transfer problem. As already mentioned, the Fe II model atom described here includes more than 13,000 individual non-LTE lines plus a large number of weak background transitions. Classical techniques, such as the complete linearization or the equivalent two-level atom methods, are computationally prohibitive. In addition, we are also interested in modeling moving media; therefore, approaches such as Anderson’s multigroup scheme or extensions of the opacity distribution function method (Hubeny & Lanz 1995) cannot be applied. Again, simple approximations such as the Sobolev method are very inaccurate in problems in which lines overlap strongly and make a significant continuum contribution (important for weak lines), as is the case for nova (and SN) atmospheres (see Paper I).

Therefore, we use the multilevel operator splitting method described by H93. This method solves the nongray, spherically symmetric, special relativistic equation of radiative transfer in the comoving (Lagrangian) frame using the operator splitting method described in Hauschildt (1992, hereafter H92). It has the advantages that (a) it is numerically highly efficient and accurate, (b) it treats the effects of overlapping lines and continua (including background opa-

cities by lines and continua not treated explicitly in non-LTE) self-consistently, (c) it gives very stable and smooth convergence even in the extreme case of novae, and (d) it is not restricted to a certain application but can be applied to a wide variety of astrophysical problems. Details of the method are described in H92 and H93, so we give here only a summary of the purely technical improvements necessary to make the non-LTE treatment of very large model atoms more efficient.

3.4. Full Non-LTE Treatment: Primary (Strong) Lines

Even with highly effective numerical techniques, the treatment of possibly more than 10^6 non-LTE lines poses a significant computational problem, in particular in terms of memory usage. In addition, most lines are very weak and do not contribute significantly to the radiative rates. However, together, they can influence the radiation field from overlapping stronger transitions and should be included as background opacity. Therefore, we separate the stronger “primary” lines from the weaker “secondary” lines by defining a threshold in $\log(gf)$ which can be arbitrarily changed. Lines with gf -values larger than the threshold are treated in detail, i.e., they are fully included as individual transitions in the radiative transfer (assuming complete redistribution) and rate equations. In addition, we include special wavelength points within the profile of the strong primary lines.

The secondary transitions are included as background non-LTE opacity sources but are not explicitly included in the rate equations. Their cumulative effect on the rates is included, since the secondary lines are treated by line-by-line opacity sampling in the solution of the radiative transfer equation. Note that the distinction between primary and secondary transitions is only a matter of convenience and technical feasibility. It is *not* a restriction of our method or the computer code and can be easily changed by altering the appropriate input files. As more powerful computers become available, all transitions can be handled as primary lines by simply changing the input files accordingly.

In a typical calculation, we use a threshold of $\log(gf) = -3$ so that lines with gf -values larger than this value are treated as primary lines and all other lines are treated as secondary lines. We do not pose additional thresholds such as the energy or the statistical weight of the lower level of a line. However, we include in the selection process only observed lines between known levels in order to include only lines with well known gf -values. All predicted lines of Kurucz are included as secondary lines (see below).

Using this procedure to select our model atom, we obtain 13,675 primary non-LTE lines between the 617 levels included in non-LTE. For Fe II lines with $\lambda > 3500 \text{ \AA}$, we use five to 11 wavelength points within their profiles. In extensive test calculations, we have found that Fe II lines with $\lambda < 3500 \text{ \AA}$ do not require these additional wavelength points in their profiles because of the fine wavelength grid used in the model calculations at these wavelengths (HB95). This procedure typically leads to about 30,000 wavelength points for the model iteration and the synthetic spectrum calculations. We show later in this paper that this wavelength grid is sufficiently dense for the calculations by comparing these results with those obtained using about 90,000 wavelength points. This is mostly because of the properties of the Fe II ion, in particular that its lines are concentrated

mostly in the wavelength range below 3500 Å. Other model atoms, e.g., Ti I, require additional wavelength points for practically every line (Hauschildt et al. 1996). For all primary lines, the radiative rates and the “approximate rate operators” (see H93) are computed and included in the iteration process.

3.5. Approximate Non-LTE Treatment: Secondary Lines and LTE Levels

The vast majority of the 1.2×10^6 Fe II lines in the database of Kurucz are either very weak lines or are predicted lines (sometimes between predicted or autoionizing levels). Although these weak lines may be a nonnegligible contribution to the overall opacity and the shape of the resulting “pseudocontinuum,” they are not very important for the rate equations. The transitions between the bound states are dominated by the fewer primary transitions, which we include individually in the radiative transfer and rate equation solution.

However, the “haze” of weak secondary lines is included as background opacity (and hence indirectly in the rate equations). This is also true for the numerous lines of species considered in LTE. Neglecting the line blanketing may lead to wrong results for the non-LTE departure coefficients; see, e.g., Hauschildt & Ensmann (1994) for a description of this effect in supernova model atmospheres.

Therefore, we include the opacity of the secondary lines, defined as all available Fe II lines that are not treated as primary lines, as background opacity. We distinguish between:

1. Lines for which the lower level is a non-LTE level but the upper level is an LTE level;
2. Lines for which the upper level is a non-LTE level but the lower level is an LTE level; and
3. Lines for which both levels are LTE levels.

Here “non-LTE” is a level that is explicitly treated in the non-LTE rate equations, whereas an “LTE level” is not considered explicitly in the rate equations. In the first two cases, we set the departure coefficient for the LTE level equal to the departure coefficient of the ground state, whereas in the third case we use the same approach as for the lines of LTE species (Baron et al. 1994; Hauschildt et al. 1994a, b), except that we use the ground-state departure coefficient to include the effects of over- or underionization. This approximate treatment of the secondary lines does not significantly influence the emergent spectra, as the secondary lines are by definition only relatively weak lines. We have verified in test calculations (HB95) that the influence of the secondary lines is indeed negligible for all models presented here. However, they are included, for completeness, in the models discussed in this paper.

3.6. The Nova Atmosphere Model

The details of our numerical assumptions and parameterization of nova atmospheres are discussed in Paper I; therefore, we give here only a short summary. The radial dependence of the density in the nova atmosphere is assumed to follow a power law $\rho \propto r^{-N}$ with a power-law index $N \approx 3$. Such a relatively flat (compared to stars and supernovae) density gradient is valid for novae in the optically thick wind phase. In addition, the atmosphere is assumed to be spherically symmetric, which is a necessary assumption to make the problem tractable. We compute the

temperature structure using radiative equilibrium in the comoving frame. All models reported here are self-consistent solutions of the radiative transfer, energy, and rate equations and iterated to full convergence. The most important model parameters are the density exponent N , the effective temperature T_{eff} , the maximum expansion velocity v_{max} , and the elemental abundances. The velocity field inside the atmosphere is computed with the condition $\dot{M}(r) = \text{const}$. While the luminosity, L , of the nova is a formal parameter of our models, it does not significantly affect the synthetic spectra (see Paper I).

4. RESULTS

Using the methods described in the previous sections, we have recomputed our nova model atmosphere grid for $L = 50,000 L_{\odot}$, $v_{\text{max}} = 2000 \text{ km s}^{-1}$, $N = 3$, solar abundances, and a set of effective temperatures from 10,000 to 60,000 K. These models include not only non-LTE for Fe II, but also for H I, He I, O I, Mg II, Ne I, and Ca II. The models were computed with our generalized model atmosphere code PHOENIX, version 5.7. For a detailed description of the code and the input physics, see Paper I. In the following discussion, we will only consider a subset of four effective temperatures, namely, 10,000, 15,000, 20,000, and 25,000 K. These effective temperatures are representative of the early evolution of a nova, and these models are sufficient to understand the basic non-LTE effects of Fe II in novae.

4.1. Non-LTE Effects on the Fe II Ionization

In Figure 2 we display the ground-state departure coefficients, b_1 , for these four nova models. We have marked the b_1 for Fe II with connected “plus” signs for clarity. In all models, the departures from LTE are significant. This is in particular true for Fe II, which shows the largest deviations from LTE in the ground state of all the species shown. However, it is interesting to note that Ca II exhibits a behavior very similar to Fe II, at least for $T_{\text{eff}} < 20,000 \text{ K}$.

For most regions of the nova atmospheres, the Fe II b_1 values are smaller than unity. This indicates an overionization of Fe II relative to LTE. Other species do not show this behavior, e.g., the ground-state departure coefficients for Ne I tend to be larger than one for most models and drop below unity only in the outermost regions of the nova atmosphere. This is likely due to both the low-ionization energy of Fe II as well as the extreme complexity of the Fe II ion. These regions mark the transition from the nova atmosphere to the nebula that is formed by the ejecta. In Figure 3 we display the ionization structure of iron throughout the atmosphere for the model with $T_{\text{eff}} = 20,000 \text{ K}$. In Figure 3a we show the non-LTE Fe II results, whereas Figure 3b shows the results for Fe II treated in LTE (but otherwise the same model structure). First note the large number of iron ionization stages that are present in the atmospheres (in a number of interleaved “Strömgren spheres”). This is a well-known feature of nova atmospheres which is caused by the large temperature gradients inside the expanding shell. We find similar effects for all elements that are included in the model calculations.

The effects of non-LTE on the Fe II ionization balance become clear by comparing Figures 3a and 3b. In the LTE case, Fe III (the dominant ionization stage of iron in the outer atmosphere) recombines to Fe II outside $\tau_{\text{std}} \approx 10^{-4}$. This causes strong Fe II lines to appear in synthetic spectra with LTE Fe II; see below. In the non-LTE Fe II case,

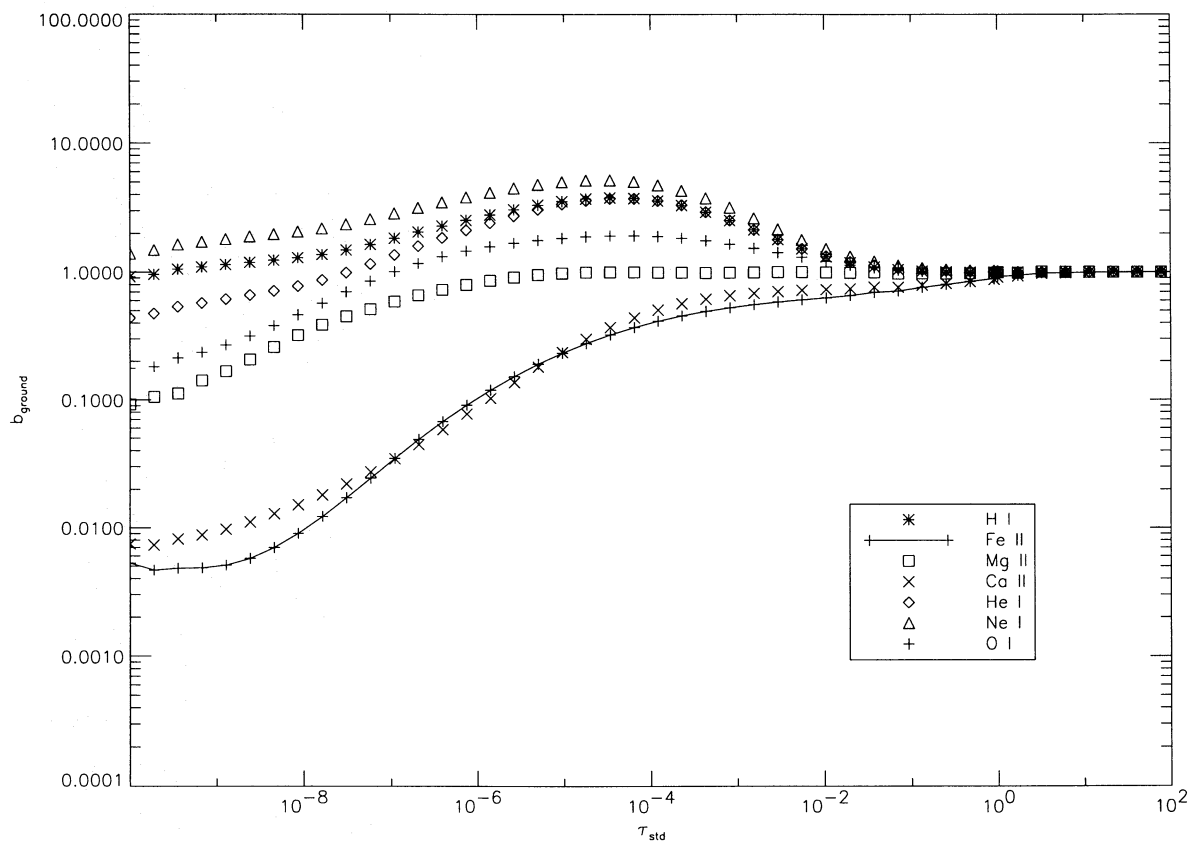


FIG. 2a

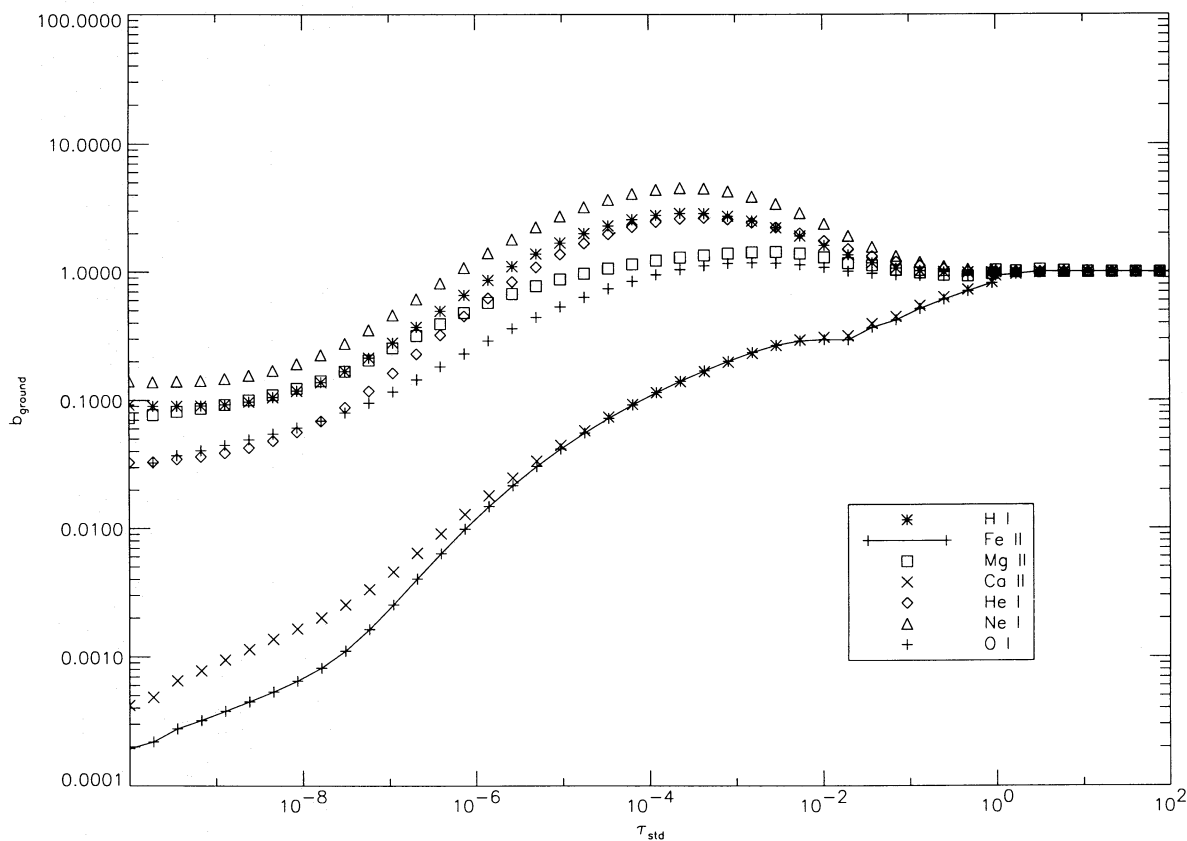


FIG. 2b

FIG. 2.—The run of the ground-state departure coefficients b_1 for the non-LTE species as functions of τ_{std} (the bound-free optical depth at 5000 Å). The different panels show the results obtained for models with effective temperatures of (a) 10,000 K, (b) 15,000 K, (c) 20,000 K, and (d) 25,000 K. The common model parameters are $L = 50,000 L_{\odot}$, $N = 3$, $v_{\text{max}} = 2000 \text{ km s}^{-1}$, and solar abundances.

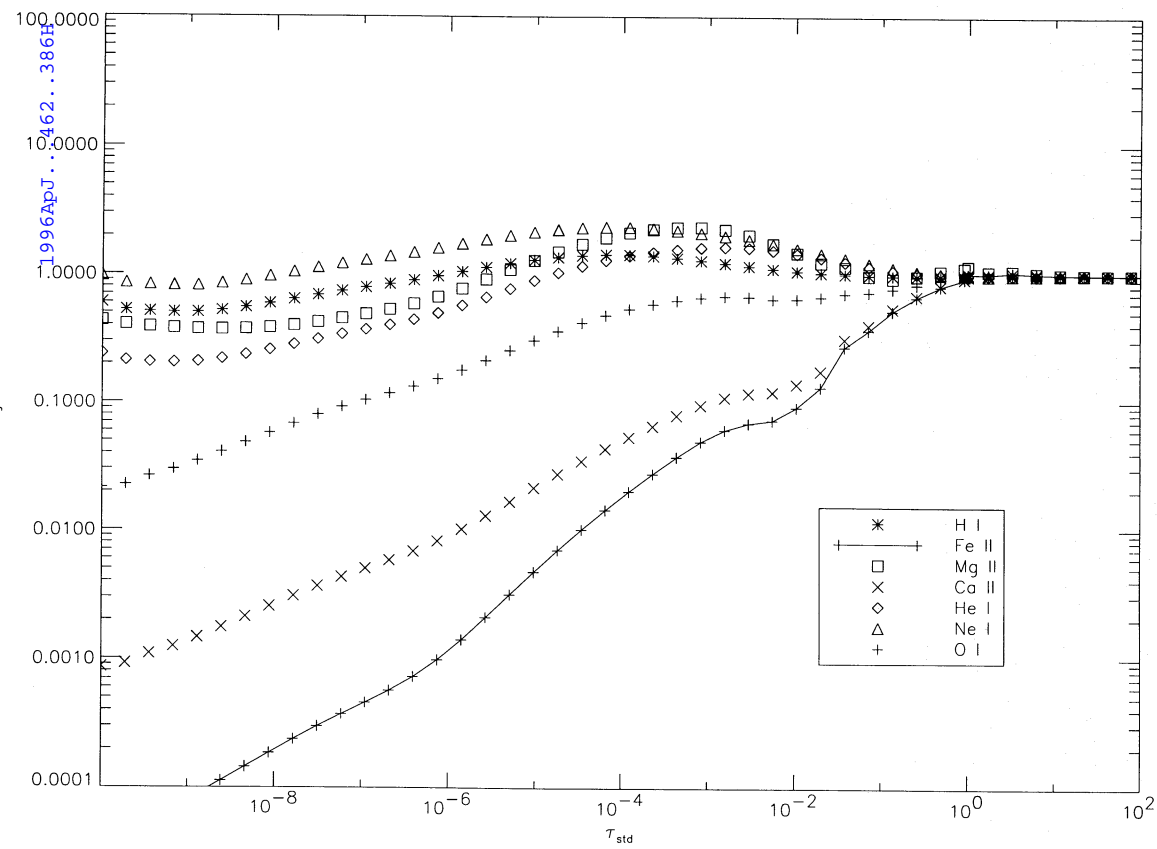


FIG. 2c

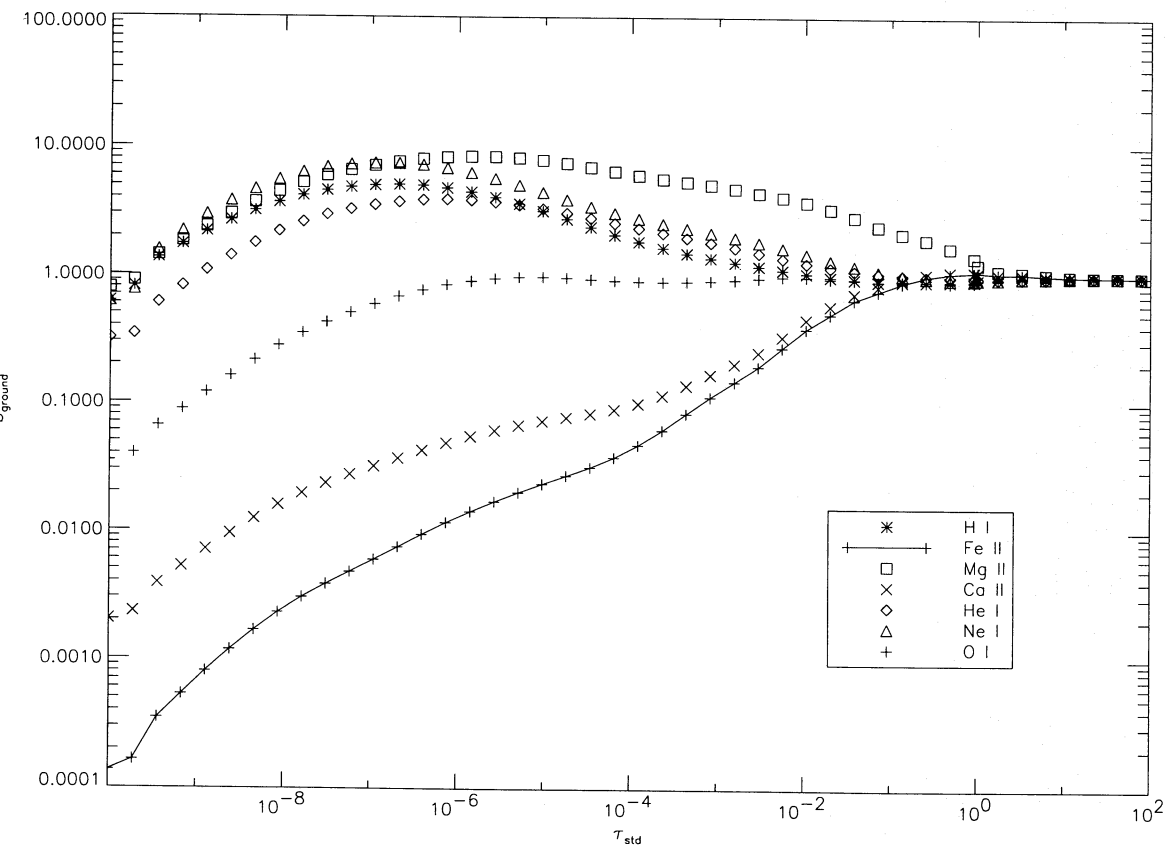


FIG. 2d

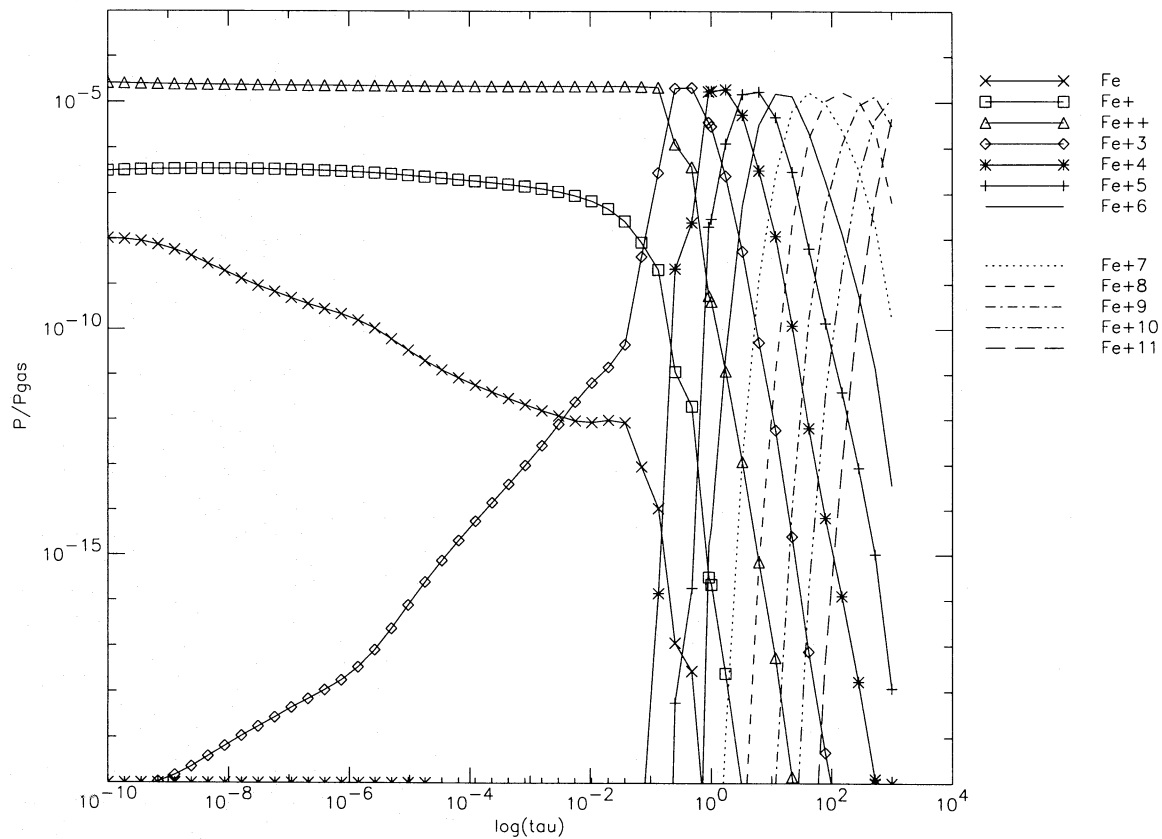


FIG. 3a

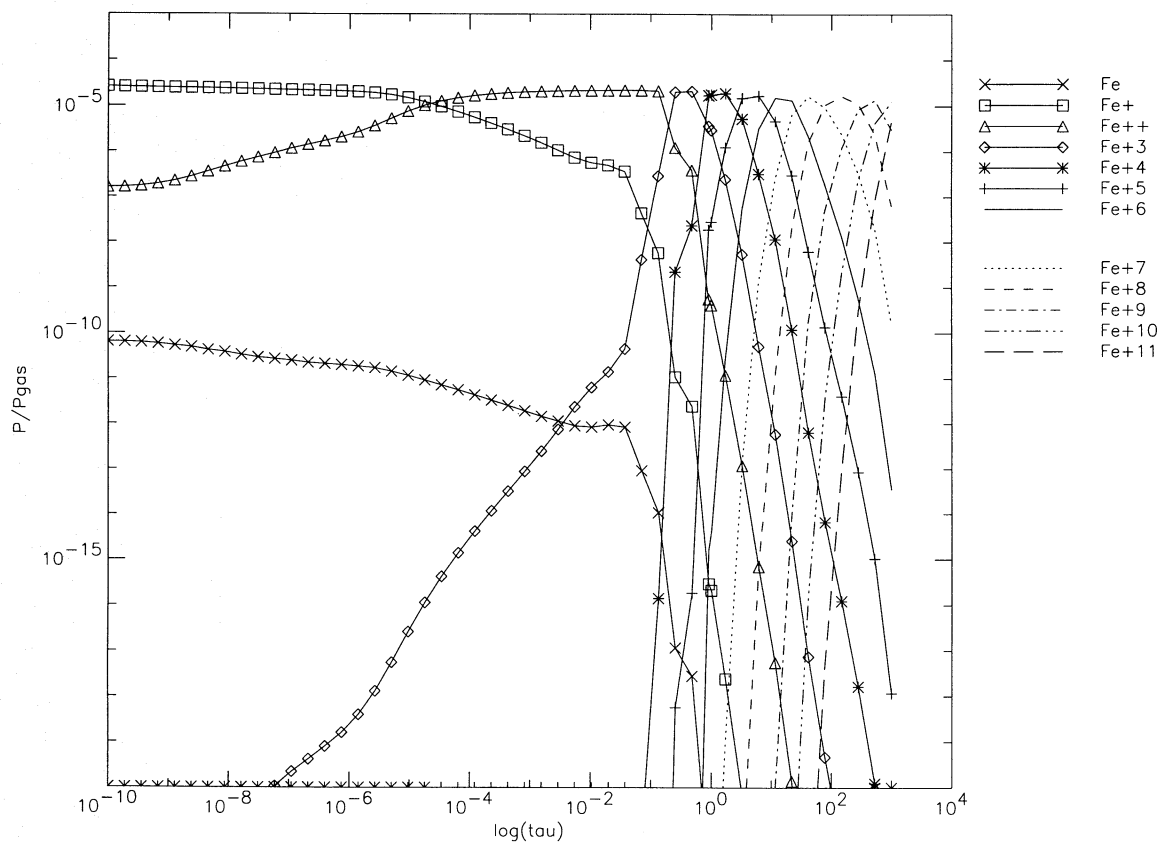


FIG. 3b

FIG. 3.—Ionization structure of iron as a function of τ_{std} (the bound-free optical depth at 5000 Å). (a) Results obtained with Fe II treated in non-LTE; (b) results for LTE Fe II. The non-LTE overionization keeps the Fe III from recombining to Fe II in the outer layers of the nova atmosphere. Note the large number of Strömgren spheres” of various ionization stages of iron in the inner parts of the nova atmosphere.

however, the strong UV radiation field prevents Fe III from recombining into Fe II throughout the outer atmosphere. This is a very important change, and it results in significantly weaker Fe II lines than found in the Fe II LTE models. We will discuss the observational implications of these results later in more detail.

The ground-state departure coefficients of all species show a complicated behavior for $0.01 \leq \tau_{\text{std}} \leq 1$, and this is very obvious in the model for $T_{\text{eff}} = 20,000$ K. This is caused by the presence of a number of ionization zones, He I to He II, He II to He III, and O III to O IV, in this region of the atmosphere (see Fig. 4). This requires the departure coefficients to change very rapidly, as they depend sensitively on the degree of ionization of the species and the electron density. Therefore, we show in Figure 5 the ratio $p(\text{Fe II})/p(\text{Fe III})$ (curve marked with plus-symbols, left-hand axis) and the ratio $p_{\text{elec}}/P_{\text{gas}}$ (dotted curve, right-hand axis) on the same graph. The sudden changes in the electron pressure (triggered mainly by the two helium ionization zones), in combination with the rapid changes in the degree of iron ionization, cause the behavior of the departure coefficients.

In Figure 6 we show the departure coefficients for all Fe II levels for the four models in an overview graph. This figure demonstrates that the non-LTE effects for Fe II become more important with higher effective temperatures. For each T_{eff} , the departure coefficients are closer to unity (their LTE value) for the higher lying levels, which are more strongly coupled to the continuum than the lower lying levels. The rather large variation of the b_i within the Fe II model atom indicates that the Fe II lines will show significant non-LTE effects themselves, in addition to the effects introduced by the changes in the ionization structure.

4.2. Non-LTE Effects on the Formation of Fe II Lines

The non-LTE effects not only change the ionization balance of iron but also change the level populations of Fe II. We demonstrate this effect for a number of important Fe II multiplets. In Figure 7 we show the ratio of the line source functions S_L to the local Planck function for the UV1 multiplet of Fe II. These are UV lines (around 2600 Å) from the ground a^6D term to z^6D^o . In the model with $T_{\text{eff}} = 15,000$ K (Fig. 7a), the UV1 multiplet is nearly in LTE in the outer atmosphere. Only between $\tau_{\text{std}} = 10^{-2}$ and 1 do the line source functions differ, by about 20%, from the Planck function. This is probably caused by the ionization zone from Fe II to Fe III which occurs at these optical depths. The situation is very different for $T_{\text{eff}} = 25,000$ K (Fig. 7b). Here the line source functions are smaller than the Planck function by up to a factor of 10. In both models, the (collisional) coupling between the levels of each term is strong enough to nearly establish the same line source function to Planck function, S_L/B , ratio for all lines within the multiplet, although the electron densities are relatively low.

The subordinate Fe II multiplet 42 (a^6S to z^6P^o) shows a somewhat different behavior (see Fig. 8). The line source functions for the three primary non-LTE lines are smaller than unity throughout the line-forming region for both the $T_{\text{eff}} = 15,000$ K (Fig. 8a) and the $T_{\text{eff}} = 25,000$ K (Fig. 8b) models. The non-LTE effects are larger for the hotter model, as seen earlier for the UV1 multiplet. This shows that the non-LTE effects for Fe II are not just overionization, but that the “internal” non-LTE effects are also significant. We emphasize this point in Figure 9 by showing the S_L/B for transitions from the ground term a^6D (Fig. 9a),

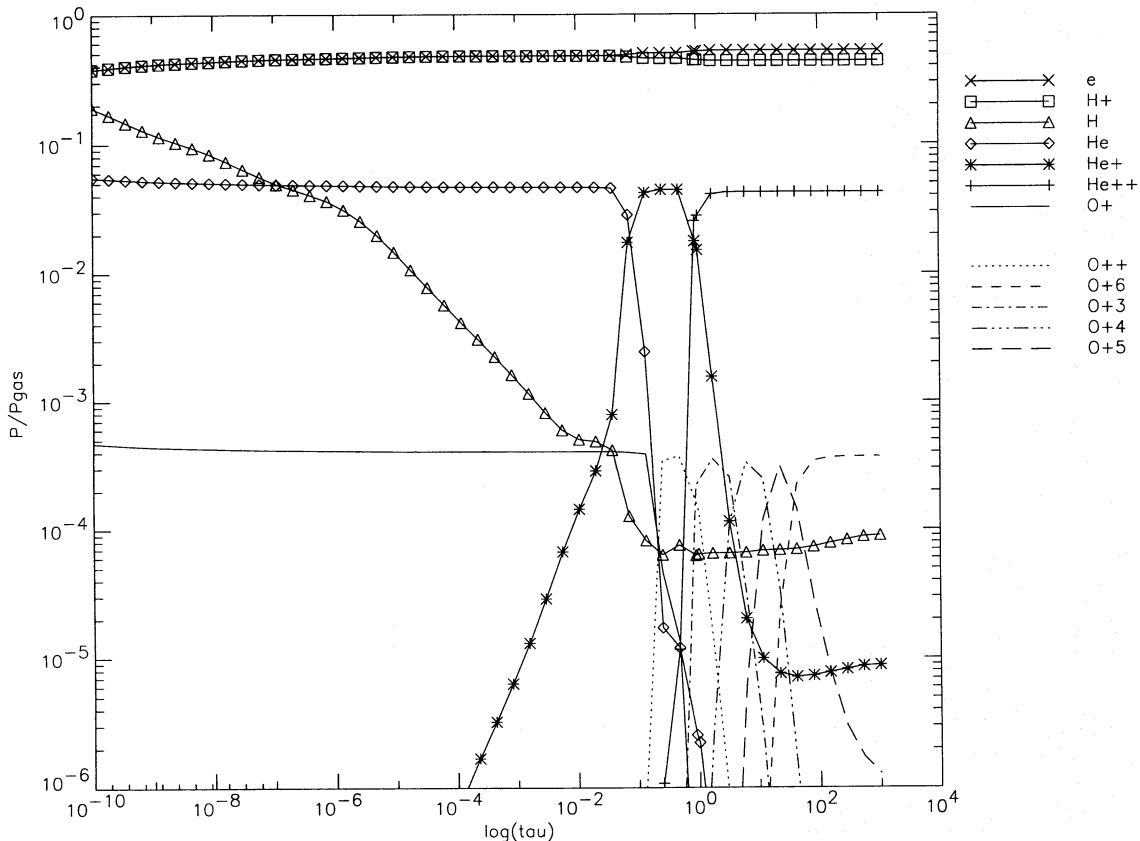


FIG. 4.—Ionization structure of the $T_{\text{eff}} = 20,000$ K nova atmosphere model as function of τ_{std} (the bound-free optical depth at 5000 Å). The graph shows the ratio of the partial pressures to the gas pressure for the 12 most abundant species.

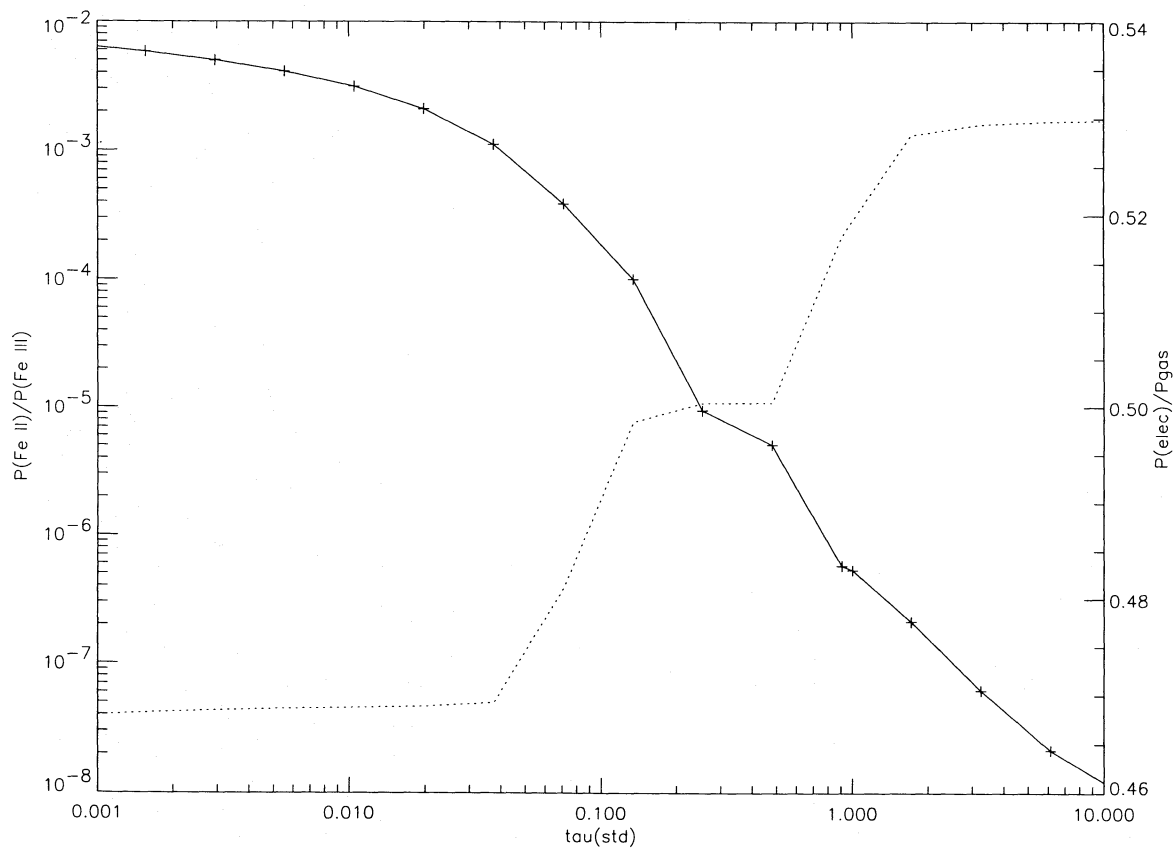


FIG. 5.—The partial pressure ratio $p(\text{Fe II})/p(\text{Fe III})$ (curve marked with plus-symbols, left-hand y-axis) and the ratio $p_{\text{elec}}/P_{\text{gas}}$ (dotted curve, right-hand y-axis) as functions of standard optical depth τ_{std} . The sudden changes in the electron pressure are caused mainly by the two helium ionization zones in combination with the rapid changes in the iron ionization degree, which is caused by the behavior of the departure coefficients.

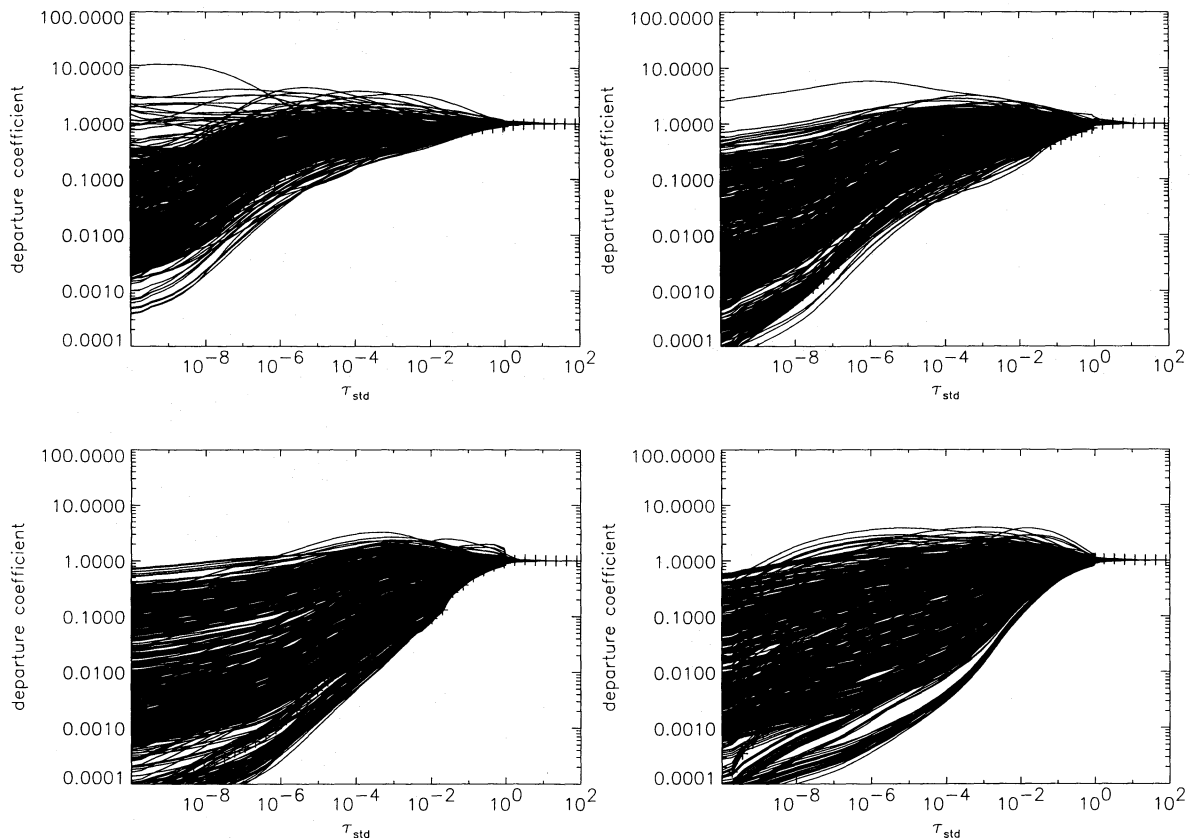


FIG. 6.—The departure coefficients for all non-LTE level of Fe II as functions of the standard optical depth τ_{std} for all four models (top left, $T_{\text{eff}} = 10,000$ K; top right, $T_{\text{eff}} = 15,000$ K; bottom left, $T_{\text{eff}} = 20,000$ K; bottom right, $T_{\text{eff}} = 25,000$ K). The plots demonstrate that the non-LTE effects become more important with higher effective temperatures. In addition, the departure coefficients are closer to unity for the higher lying levels.

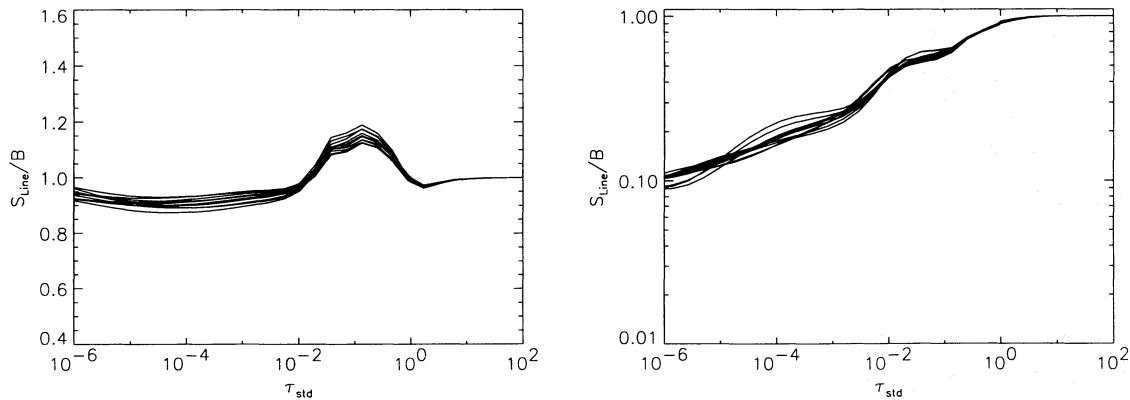


FIG. 7.—The ratio of the line source function to the local Planck function for the UV1 multiplet (a^6D to z^6D^o) as functions of the standard optical depth. The two panels are for models with (a) $T_{\text{eff}} = 15,000$ K and (b) $T_{\text{eff}} = 25,000$ K.

the metastable a^4F term (Fig. 9b), and the higher z^4P^o term (Fig. 9c) for both the 15,000 and the 25,000 K models. The general trend is that the non-LTE effects become more important for higher effective temperatures and they become less important for higher lying terms, as expected.

4.3. The Effects of Fe II Non-LTE on Nova Spectra

The results that we have described in the preceding sections indicate that the treatment of Fe II in non-LTE must have significant effects on the spectra emitted by nova atmospheres. In the following discussion, we distinguish between cooler ($T_{\text{eff}} < 20,000$ K) and hotter nova models.

4.3.1. Nova Atmospheres with $T_{\text{eff}} < 20,000$ K

For nova atmospheres with relatively low effective temperatures, we find that the effects of non-LTE on the emitted spectra are smaller than in the atmospheres with higher T_{eff} . In Figures 10 and 11 we show (a) the UV and (b) optical spectra of models with $T_{\text{eff}} = 10,000$ K (Fig. 10) and $T_{\text{eff}} = 15,000$ K (Fig. 11). In the top plot of each graph, we display the synthetic spectra computed with Fe II LTE (dotted curves) and Fe II non-LTE treatment (solid curves). In order to show the differences between the spectra in greater detail, we plot in the bottom part of each panel the relative differences between the spectra of the LTE and non-LTE Fe II models. Note that the relative differences are plotted such that a positive value indicates that the flux of the LTE model is larger than the flux emitted by the non-LTE model and vice versa.

We consider first the UV spectra. In general, the Fe II non-LTE spectrum shows slightly less flux in this spectral region than the corresponding Fe II LTE spectrum. A number of the Fe II features and blends, in particular the $\lambda 2640$ feature (this is *not* an emission line for these effective temperatures; see Hauschildt et al. 1995) and the Fe II–Mg II complex at 2800 \AA , are stronger in the Fe II non-LTE spectrum. For smaller wavelengths, i.e., the IUE short-wavelength prime range $1000\text{--}2200 \text{ \AA}$, the differences between the two spectra can be as much as a factor of 10. However, the total amount of flux emitted in the SWP range is small. The differences between LTE Fe II and non-LTE Fe II models are also relatively small in the IUE long-wavelength prime range ($2300\text{--}3200 \text{ \AA}$), but the fit to observed nova spectra is improved with the non-LTE Fe II models (Schwarz et al. 1996).

The changes between the LTE and non-LTE Fe II spectra are larger in the optical. In general, the Fe II lines are *stronger* in the non-LTE models than in the LTE models. The relative difference can be as much as 80% for the Fe II multiplet lines just longward of $H\beta$. These are significant changes and could be interpreted as abundances changes of iron by more than a factor of 2. Therefore, non-LTE effects for Fe II must be included in the analysis of the optical spectra of novae, even in the earliest stages of its evolution. The fundamental differences between the effects of non-LTE on the Fe II lines in the UV and the optical spectral ranges show that a very detailed and careful treatment of Fe II non-LTE is necessary for reliable results. Simplified treat-

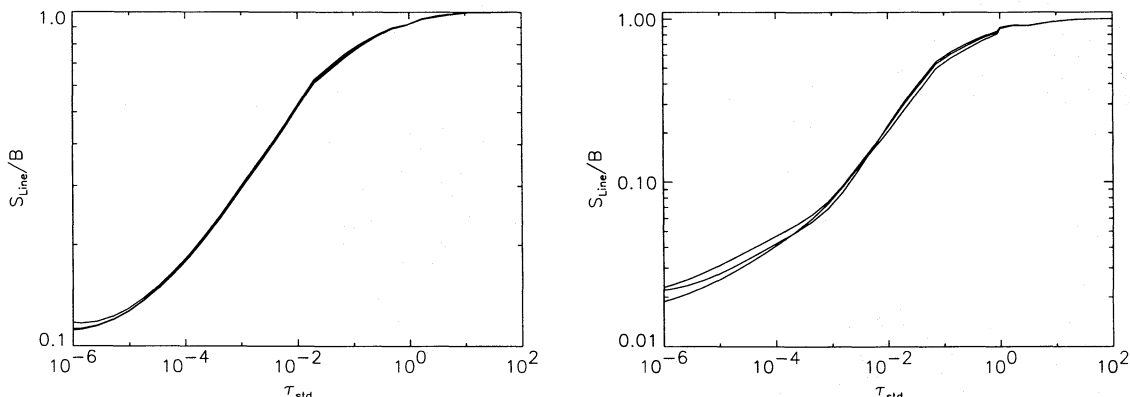


FIG. 8.—The ratio of the line source function to the local Planck function for multiplet 42 (a^6S to z^6P^o) as functions of the standard optical depth. The two panels are for models with (a) $T_{\text{eff}} = 15,000$ K and (b) $T_{\text{eff}} = 25,000$ K.

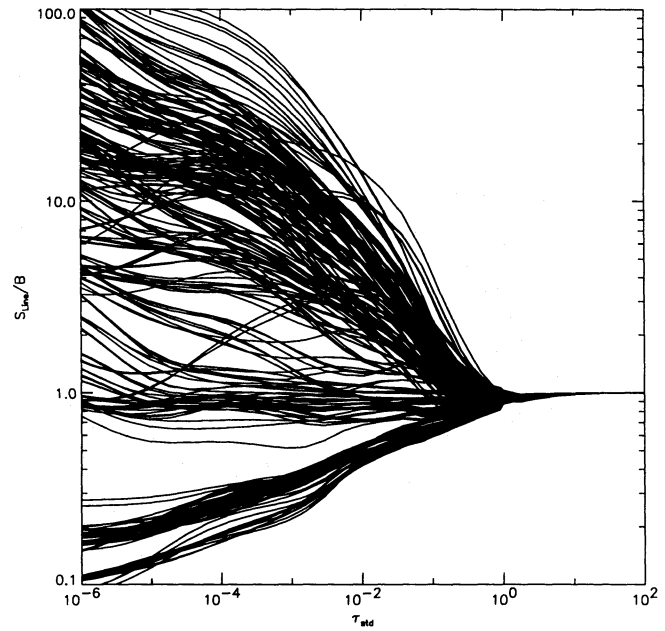
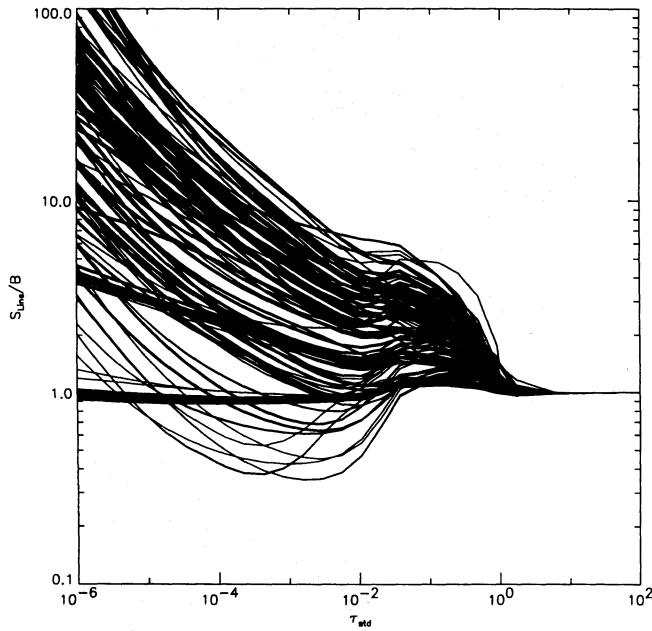


FIG. 9a

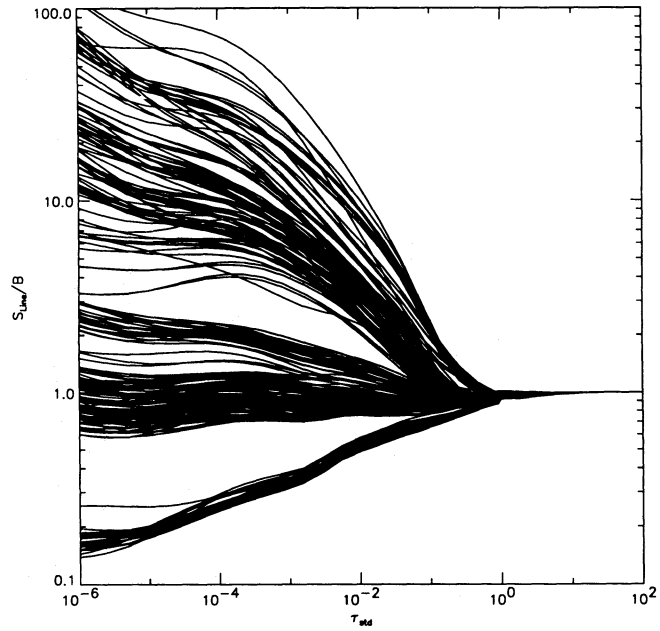
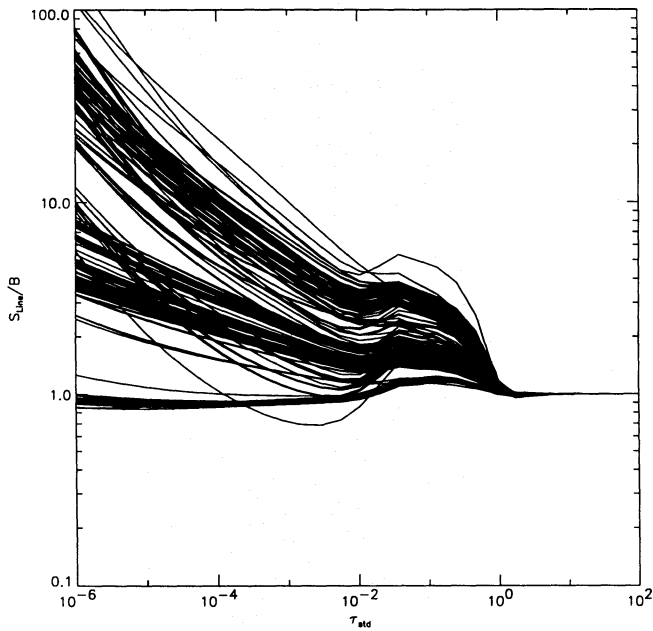


FIG. 9b

FIG. 9.—The ratio of the line source function to the local Planck function for lines originating from (a) the ground term a^6D , (b) the metastable a^4F term, and (c) the higher z^4P^o term for both the 15,000 (left) and the 25,000 K (right) models.

ments, e.g., assuming ionization corrections but “internal” LTE (i.e., assuming that $b_i = b_j$ for $i \neq j$) for Fe II, may lead to wrong conclusions.

4.3.2. Nova Atmospheres with $T_{\text{eff}} \geq 20,000$ K

The effect of Fe II non-LTE on the synthetic spectra is very different for higher effective temperatures. In Figures 12 and 13 we show (a) the UV and (b) optical spectra for models with $T_{\text{eff}} = 20,000$ K (Fig. 12) and $T_{\text{eff}} = 25,000$ K (Fig. 13); the different parts of the figures and the meaning of the line styles are the same as above. The changes in the UV spectra are now very large. The Fe II LTE spectra predict very strong Fe II lines. In fact, they would be the strongest lines in the UV spectrum if the assumption of LTE

was valid for Fe II. That this is not the case is obvious from the corresponding non-LTE Fe II spectrum. The Fe II lines that dominated the UV spectrum in the LTE Fe II model are reduced to near invisibility in the non-LTE model. This is especially true for the Fe II lines in the wavelength range from 2400 to 2800 Å (including the Fe II–Mg II blend at 2800 Å). It is clear that the assumption of LTE for Fe II has completely broken down and that non-LTE effects must be considered in order to correctly interpret the UV spectrum. The relative differences can be as much as factor of 5, and also the changes in the appearance of the spectrum are significant.

In contrast, the differences between the optical spectra of LTE Fe II and non-LTE Fe II are very small, at most 6%,

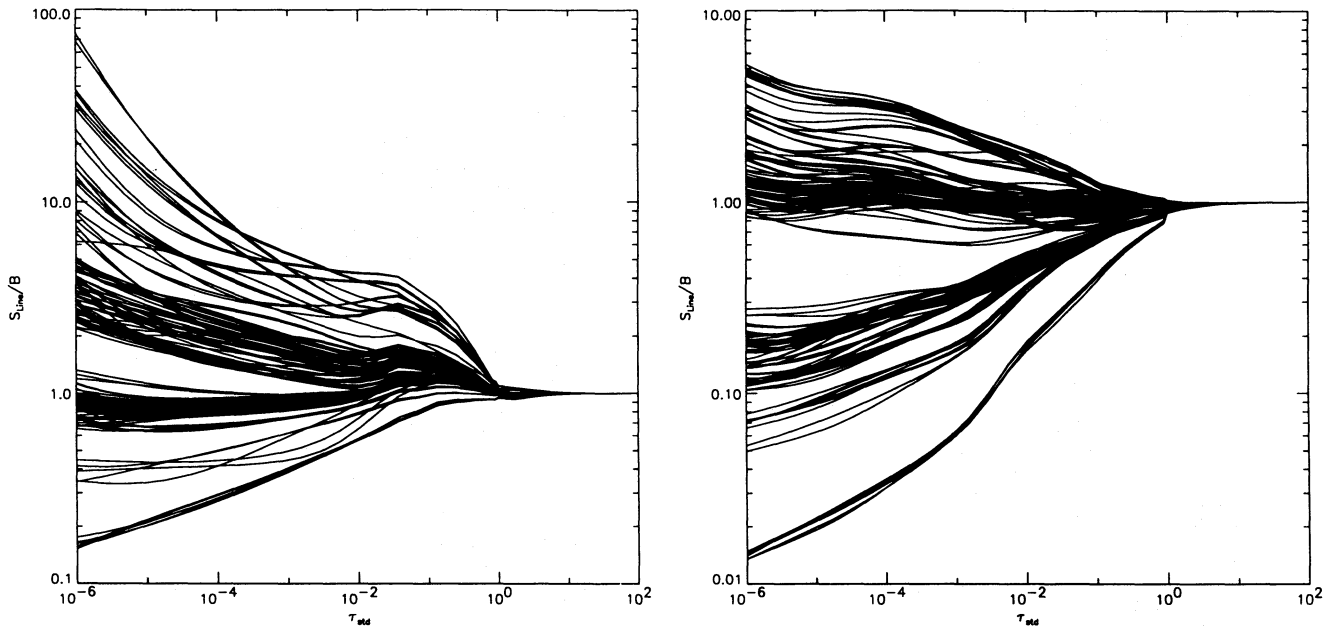


FIG. 9c

for the model with $T_{\text{eff}} = 25,000$ K. For this effective temperature, the optical Fe II lines are already weak, and thus the non-LTE effects on Fe II cannot change the emitted spectrum significantly. The model with $T_{\text{eff}} = 20,000$ K shows differences of up to 20%. As for the UV spectrum, and contrary to the situation at lower T_{eff} , the non-LTE Fe II lines are now weaker than in the LTE case. The non-LTE effects on the Fe II line formation are also significant in the optical ranges and, again, they could be *wrongly* interpreted as abundance changes. In the case of novae, where abundance changes of iron are possible due both to mixing of core material with accreted material and to CNO nuclear reactions (actually depletion of hydrogen), this is a very important fact.

4.4. Result of Test Calculations

We mentioned earlier in this paper that additional wavelength points for the Fe II lines below 3500 \AA are not required for the model calculations. This is because the UV lines of Fe II occur in dense clusters which can be modeled accurately by our already fine wavelength grid. To verify this, we have performed full model calculations with five additional wavelength points for every primary Fe II line, leading to a total of 90,000 wavelength points. We have compared the ground-state departure coefficients for the 15,000 and the 25,000 K models computed with either 90,000 wavelength points (five points per primary non-LTE line plus default wavelength points) or 25,000 wavelength points (default wavelength points and no additional wavelength points for Fe II lines below 3500 \AA). The differences in the ground-state departure coefficients are less than the accuracy required for the iterations (1%), and it is clear that the departure coefficients are independent of the number of wavelength points (for our choice of the regular wavelength grid). Finally, in Figure 14 we compare the synthetic spectra computed for the 90,000 wavelength point models (*solid curves*) with the spectra computed for the 25,000 wavelength point models (*dotted lines*) for the $T_{\text{eff}} = 15,000$ K model. The differences are very small in these spectra and can hardly be seen in the plots. This shows that our smaller

wavelength grid can be used for the model calculations, fully resolving the cores and the wings of the lines, resulting in savings of a factor of 3 in total computer time. The smaller wavelength grid, however, can only be used because of the properties of the Fe II ion, for other large non-LTE ions, e.g., Ti I (Hauschildt et al. 1996), the large-wavelength grid may be required for model calculations. This results only in longer model calculations (a complete model calculation [20 iterations] with 90,000 wavelength points takes about 12,000 s of CPU time on one Cray C90 processor) but does *not* require more storage or memory. Therefore, even model calculations with 90,000 wavelength points do not pose any technical problem and can be done on high-end workstations.

5. SUMMARY AND CONCLUSIONS

In this paper, we have for the first time reported on nova model atmosphere calculations done with a new and detailed non-LTE treatment for Fe II. Our model atom includes 617 levels and 13,675 primary transitions. The model atmospheres are fully self-consistent solutions of the nongray radiative transfer and energy equations and the non-LTE rate equations (including a number of other non-LTE species in addition to Fe II). We have compared the results of model calculations with 90,000 and 25,000 wavelength points (the latter especially selected to guarantee good coverage of the Fe II lines) and found insignificant differences.

We find that the non-LTE effects for Fe II are extremely important in all nova models that we have considered. The changes in the synthetic spectra are largest for higher effective temperatures ($T_{\text{eff}} \geq 20,000$ K) and, in particular, for the ultraviolet. For smaller effective temperatures, the changes in the synthetic UV spectra are smaller; however, they are significant for the analysis of optical nova spectra. Non-LTE effects are also significant for the formation of optical Fe II lines, and they must be included in interpreting the optical spectra of novae.

One of the major effects of non-LTE Fe II line formation is a strong overionization from Fe II to Fe III, caused by the

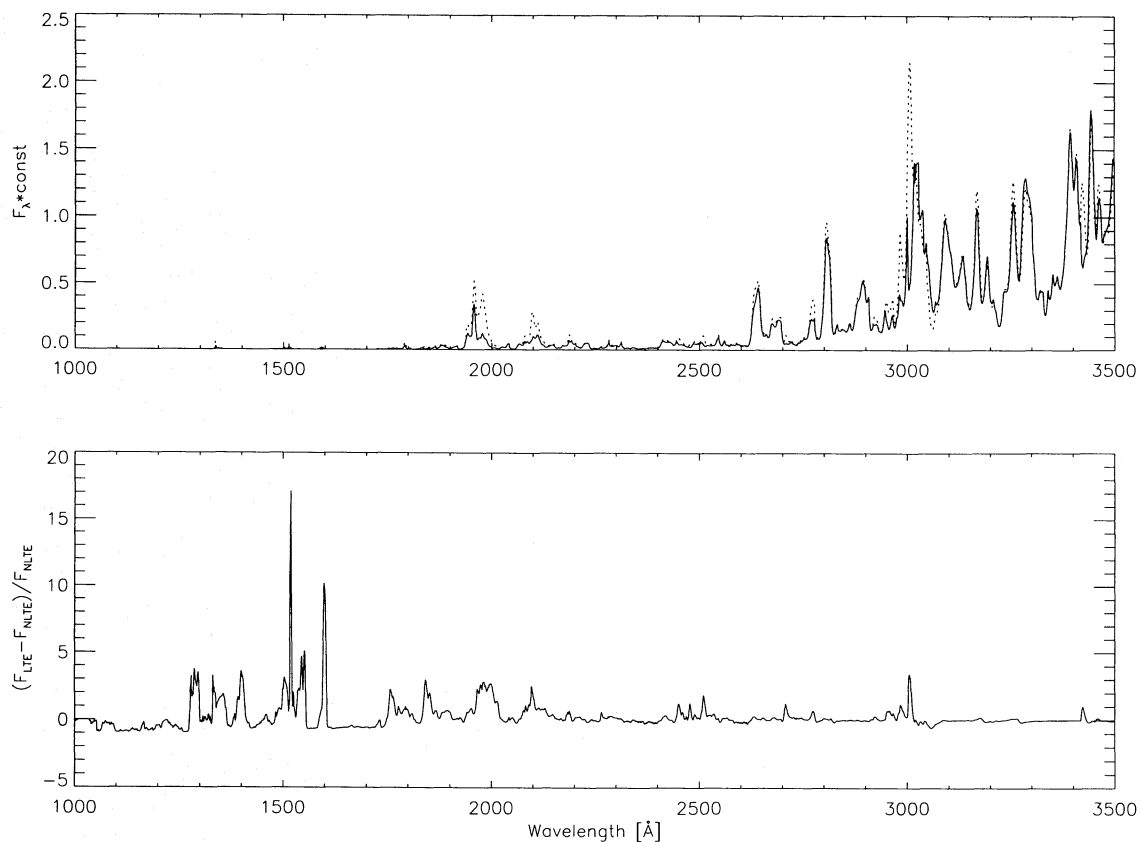


FIG. 10a

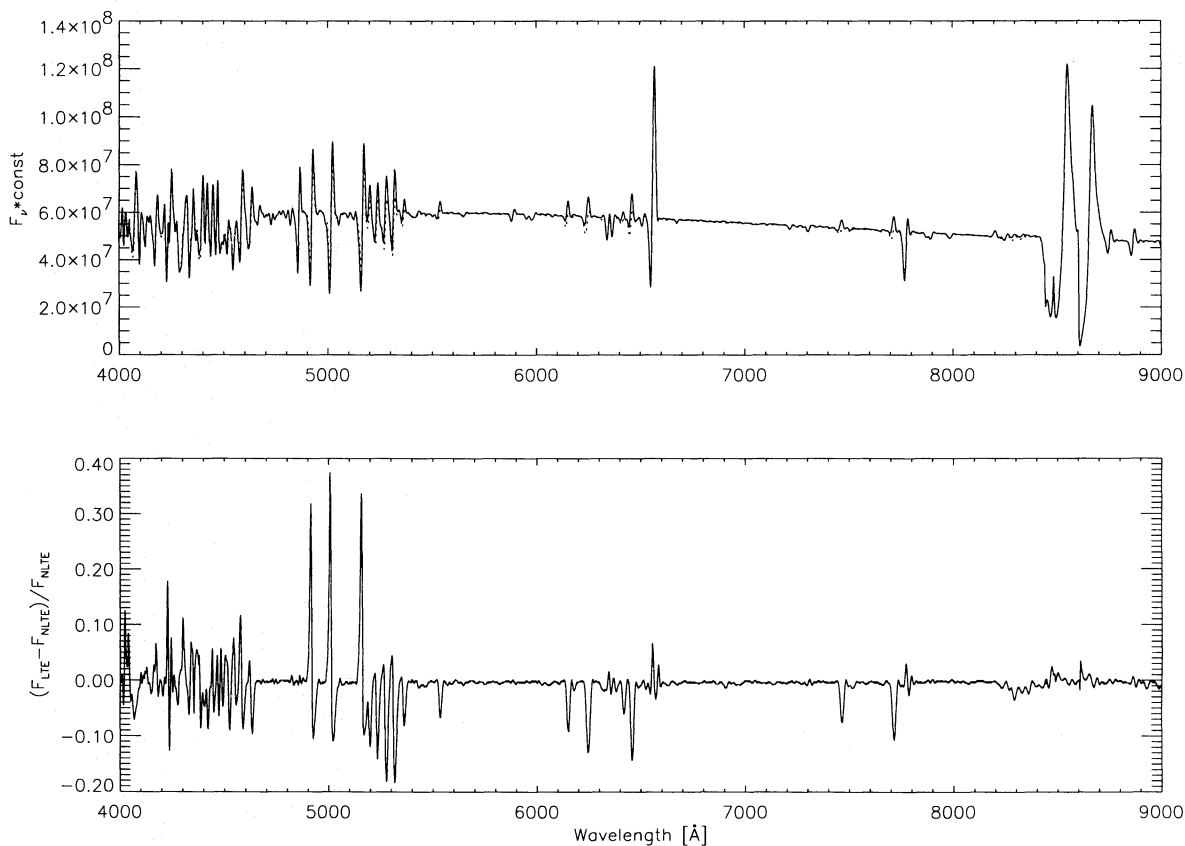


FIG. 10b

FIG. 10.—(a) UV and (b) optical spectra of models with $T_{\text{eff}} = 10,000$ K. We show the synthetic spectra for the full Fe II non-LTE treatment (*solid curves*) and for LTE Fe II (*dotted curves*). The bottom parts of each panel show the ratio of the LTE Fe II and non-LTE Fe II spectra to emphasize the difference between the spectra.

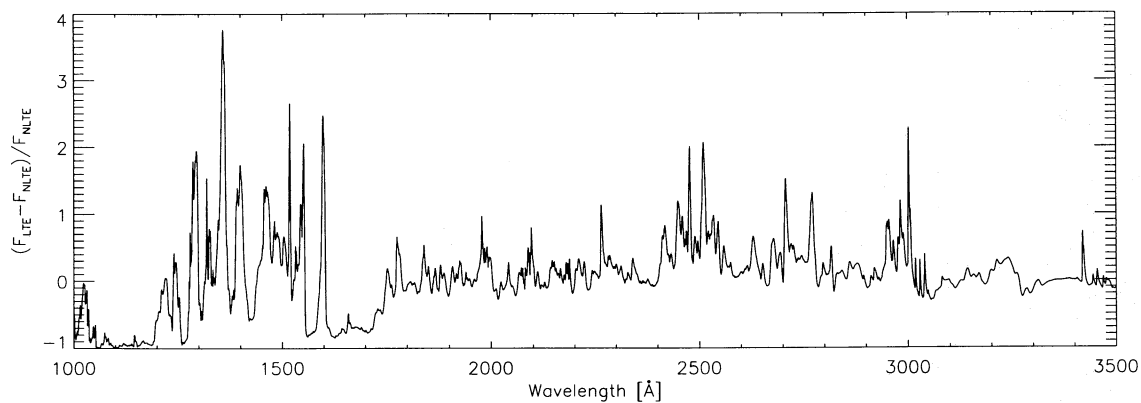
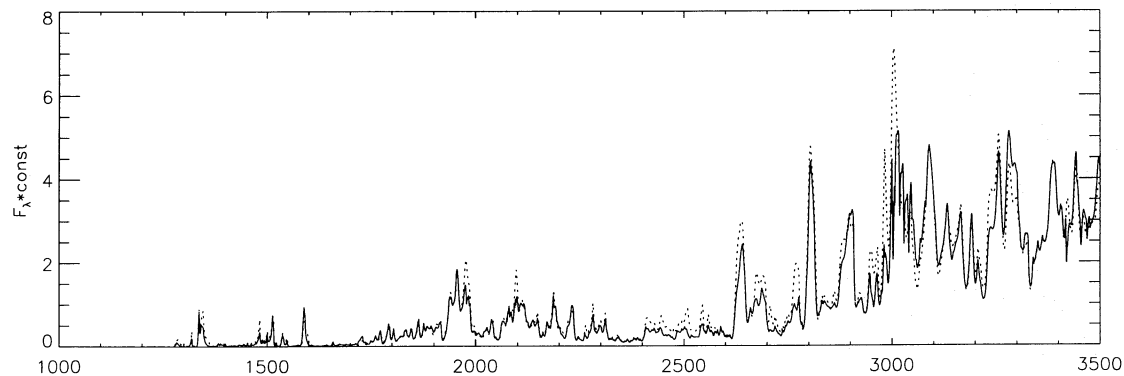


FIG. 11a

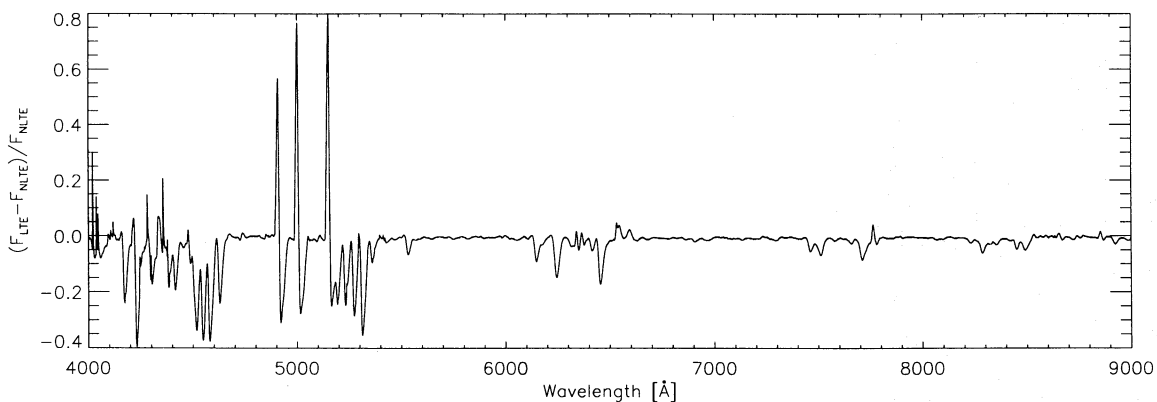
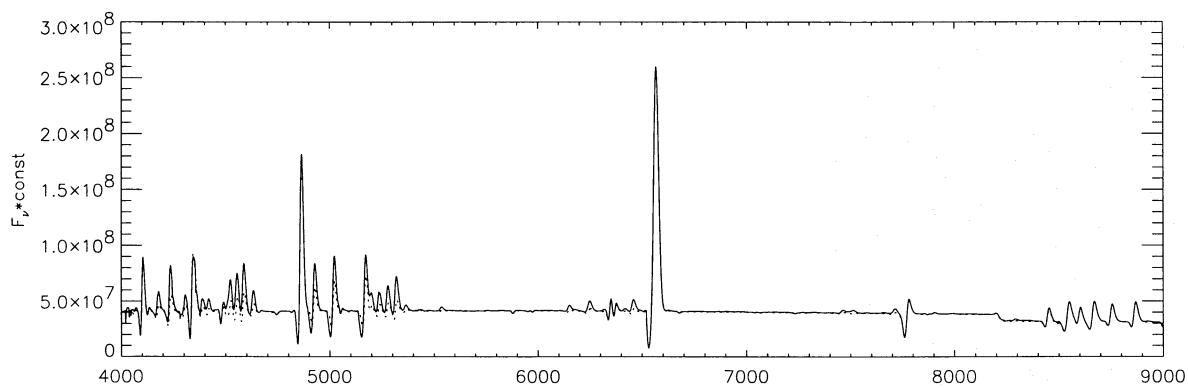


FIG. 11b

FIG. 11.—(a) UV and (b) optical spectra of a model with $T_{\text{eff}} = 15,000$ K. We show the synthetic spectra for the full Fe II non-LTE treatment (solid curves) and for LTE Fe II (dotted curves). The bottom parts of each panel show the ratio of the LTE Fe II and non-LTE Fe II spectra to emphasize the difference between the spectra.

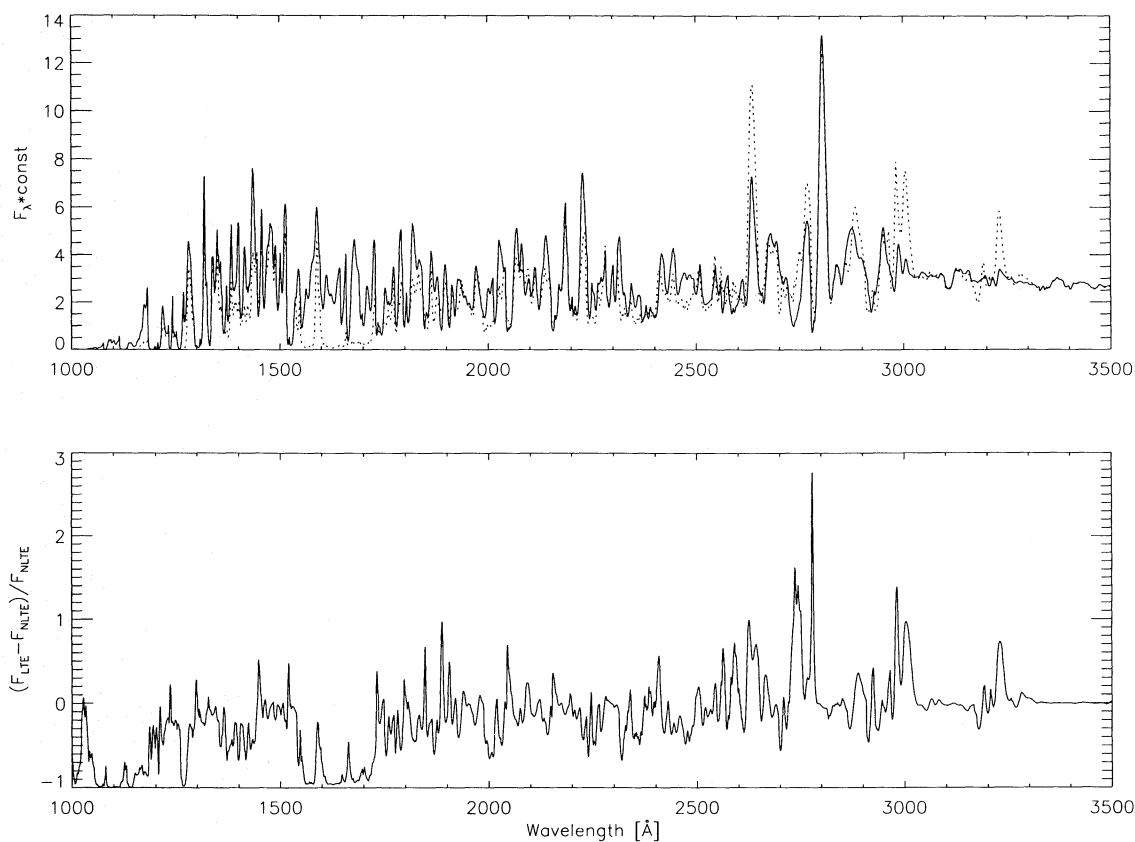


FIG. 12a

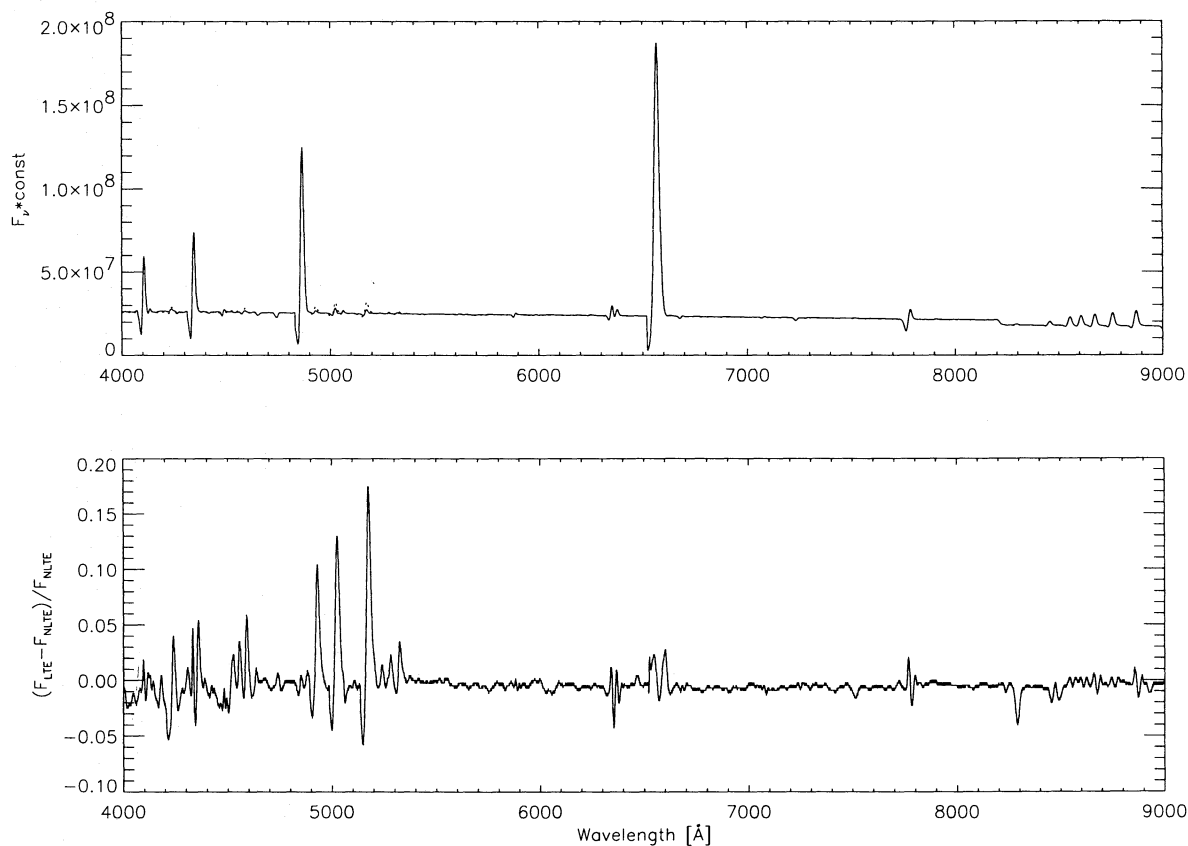


FIG. 12b

FIG. 12.—(a) UV and (b) optical spectra of models with $T_{\text{eff}} = 20,000$ K. In the top parts of the graphs, we show the synthetic spectra for the full Fe II non-LTE treatment (solid curves) and for LTE Fe II (dotted curves). The bottom parts of each panel show the ratio of the LTE Fe II and non-LTE Fe II spectra to emphasize the difference between the spectra.

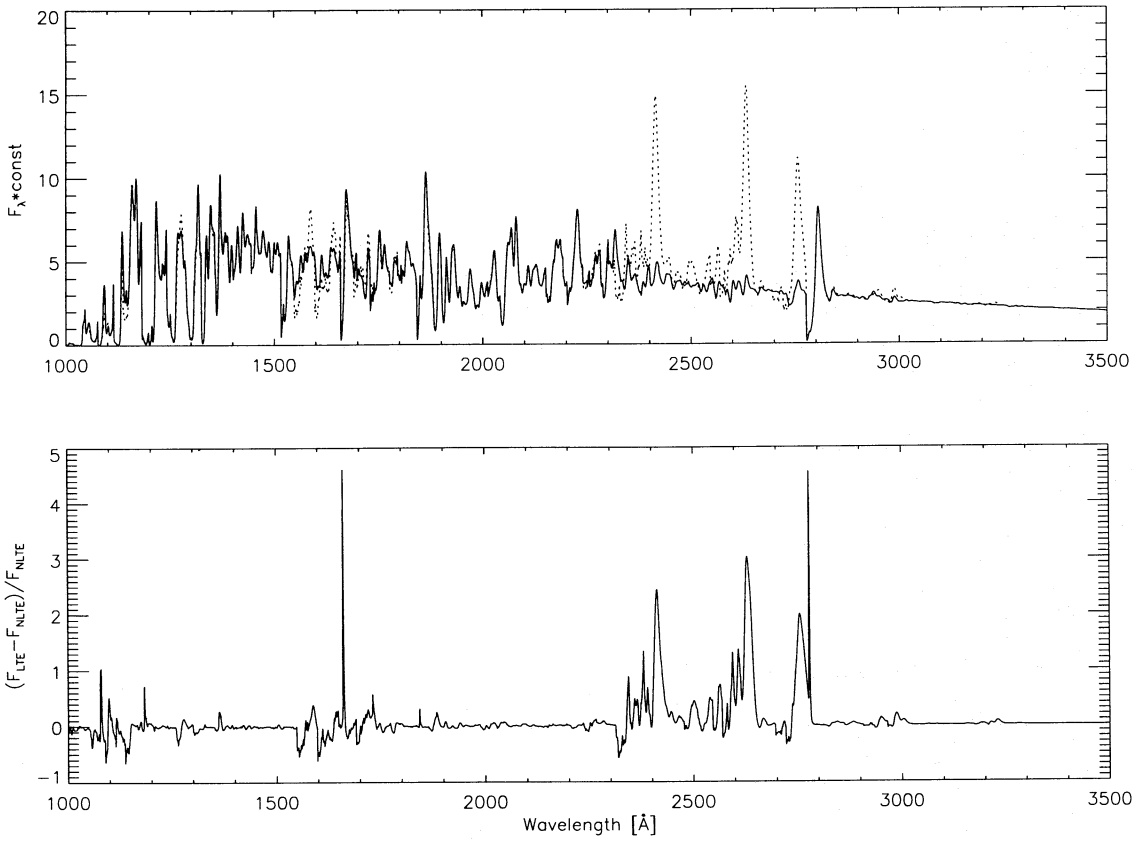


FIG. 13a

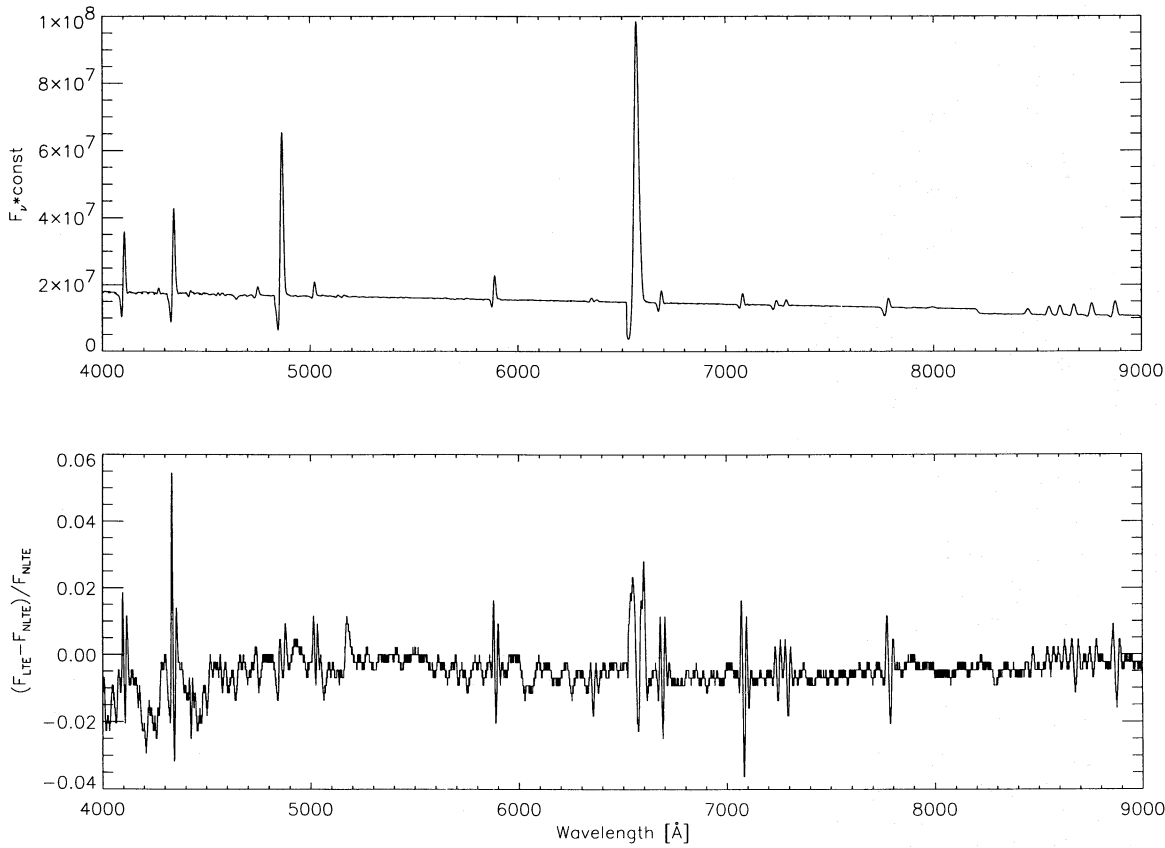


FIG. 13b

FIG. 13.—(a) UV and (b) optical spectra of models with $T_{\text{eff}} = 25,000$ K. In the top parts of the graphs we show the synthetic spectra of the full Fe II (solid curves) and for LTE Fe II (dotted curves). The bottom parts of each panel show the ratio of the LTE Fe II and non-LTE Fe II spectra to emphasize the difference between the spectra.

FIG. 13
non-LTE
to em

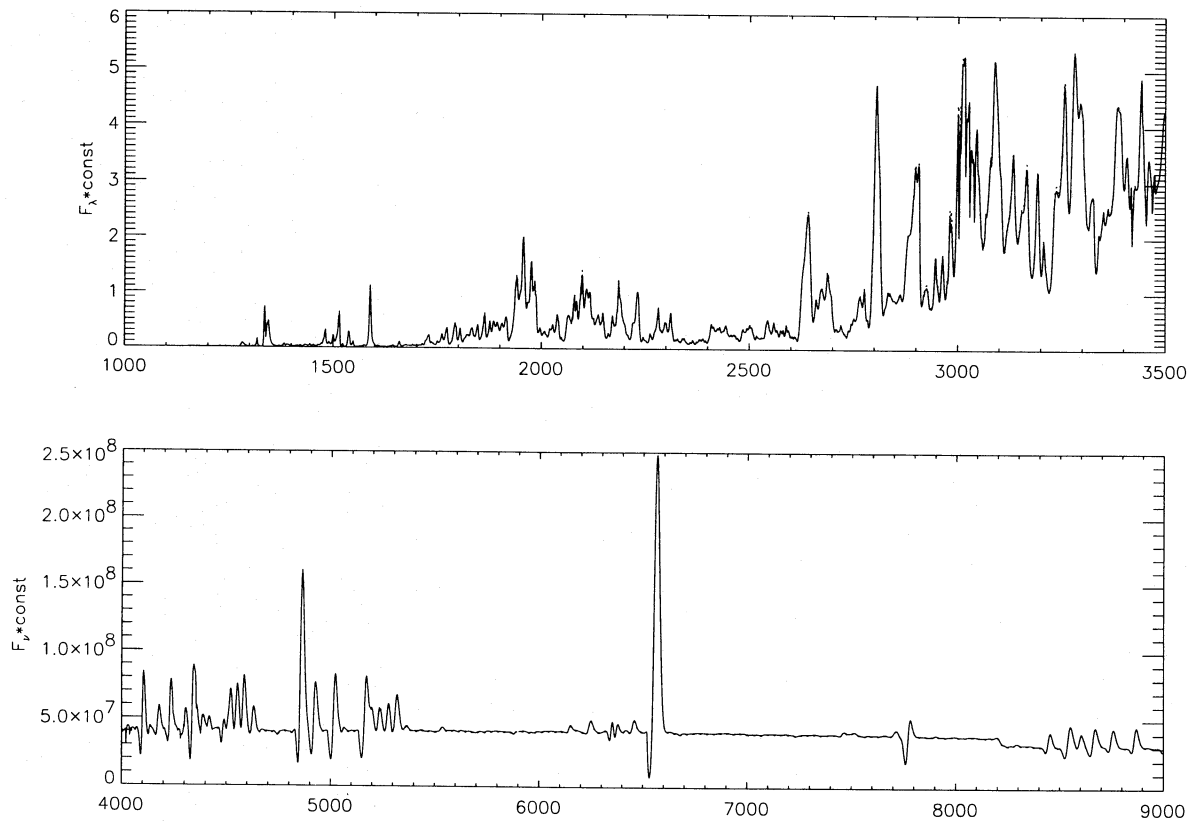


FIG. 14.—The synthetic spectra computed for a model with $T_{\text{eff}} = 15,000$ K with 90,000 wavelength points (solid curves) and 25,000 wavelength points (dotted curves) in the ultraviolet (top) and the optical (bottom). The plots demonstrate that the results of the model calculations do not depend significantly on the number of wavelength points used in the models as long as enough wavelength points are used (in this case, $\geq 25,000$ points) and are placed correctly so that the wavelength space is saturated.

strong UV radiation fields present in nova atmospheres. These radiation fields keep Fe III from recombining to Fe II throughout the atmosphere. This is an important non-LTE effect, and LTE Fe II models predict too much Fe II in the line-forming regions of nova winds.

In subsequent papers (Schwarz et al. 1996), we will show that inclusion of Fe II non-LTE leads to improved fits to the observed optical and UV spectra of novae.

It is a pleasure to thank H. Störzer, J. Krautter, and

S. Shore for stimulating discussions. This work was supported in part by NASA LTSA grants to Arizona State University, by NASA grant NAGW-2999, as well as NSF grants to Wichita State University. Some of the calculations presented in this paper were performed at the San Diego Supercomputer Center (SDSC), supported by the NSF, and at the NERSC, supported by the US DoE; we thank them for a generous allocation of computer time. The development of the PHOENIX opacity database was sponsored in part by a grant to F. A. from the American Astronomical Society.

REFERENCES

- Allen, C. W. 1973, *Astrophysical Quantities* (3d ed.; London: Athlone)
 Baron E., et al. 1994, *ApJ*, 441, 170
 Baron, E., Hauschildt, P. H., & Mezzacapa, A. 1995, *MNRAS*, in press
 Bath, G. T., & Shaviv, G. 1976, *MNRAS*, 75, 305
 Drawin, H. W. 1961, *Z. Phys.*, 164, 513
 Eastman, R. G., & Pinto, P. A. 1993, *ApJ*, 412, 731
 Hauschildt, P. H. 1992, *J. Quant. Spectrosc. Radiat. Transfer*, 47, 433 (H92)
 ———. 1993, *J. Quant. Spectrosc. Radiat. Transfer*, 50, 301 (H93)
 Hauschildt, P. H., & Baron, E. 1995, *J. Quant. Spectrosc. Radiat. Transfer*, in press (HB95)
 Hauschildt, P. H., & Ensmann, L. M. 1994, *ApJ*, 424, 905
 Hauschildt, P. H., Starrfield, S., Austin, S. J., Wagner, R. M., Shore, S. N., & Sonneborn, G. 1994a, *ApJ*, 422, 831
 Hauschildt, P. H., Starrfield, S., Shore, S. N., Allard, F., & Baron, E. 1995, *ApJ*, 447, 829 (Paper I)
 Hauschildt, P. H., Starrfield, S., Shore, S. N., Gonzales-Riestra, R., Sonneborn, G., & Allard, F. 1994b, *AJ*, 108, 1008
 Hauschildt, P. H., Störzer, H., & Baron, E. 1994c, *J. Quant. Spectrosc. Radiat. Transfer*, 51, 875
 Hauschildt, P. H., Wehrse, R., Starrfield, S., & Shaviv, G. 1992, *ApJ*, 393, 307
 Hauschildt, P. H., et al. 1996, in preparation
 Hubeny, I., & Lanz, T. 1995, *ApJ*, 439, 875
 Kurucz, R. L. 1994, *Atomic Data for Fe, Co, and Ni* (Kurucz CD-ROM No. 22)
 Mihalas, D., & Weibel-Mihalas, B. 1984, *Foundations of Radiation Hydrodynamics* (Oxford: Oxford Univ. Press)
 Reilman, R. F., & Manson, S. T. 1979, *ApJS*, 40, 815
 Schwarz, G., et al. 1996, in preparation
 Van Regemorter, H. 1962, *ApJ*, 136, 906